

DEVELOPMENT OF NMR BASED *IN VITRO* AND *IN VIVO* METHODS TO STUDY  
NUCLEOTIDE SUGAR INTERCONVERSIONS

by

PRASANTH SAMBARAJU

(Under the Direction of James H. Prestegard)

ABSTRACT

Polysaccharides are the dominant components of a plant cell wall. Chemically the plant cell wall consists of cellulose microfibrils embedded in a matrix of hemicellulose and pectin. The matrix polysaccharides are made in the Golgi from nucleotide sugars and are then exported to the cell wall. The goal of this thesis is to develop *in vitro* and *in vivo* NMR methods to study nucleotide sugar interconversions that lead to the starting products for matrix polysaccharide synthesis and to analyze the data using multivariate statistical methods. The *in vitro* method included the detection of UDP-Apiose formation from UDP-Glucuronic acid in presence of UDP-Apiose/xylose synthase. The organelle method was developed to study the interconversion of nucleotide sugars within the Golgi apparatus.

INDEX WORDS: cell wall, polysaccharides, pectin, Golgi apparatus, NMR, sugar nucleotides

DEVELOPMENT OF NMR BASED *IN VITRO* AND *IN VIVO* METHODS TO STUDY  
NUCLEOTIDE SUGAR INTERCONVERSIONS

by

PRASANTH SAMBARAJU

B.Pharmacy, Osmania University, India, 1999

M. Pharmacy, Panjab University, India, 2002

A Thesis Submitted to the Graduate Faculty of The University of Georgia in Partial  
Fulfillment of the Requirements for the Degree

MASTER OF SCIENCE

ATHENS, GEORGIA

2007

© 2007

Prasanth Sambaraju

All Rights Reserved

DEVELOPMENT OF NMR BASED *IN VITRO* AND *IN VIVO* METHODS TO STUDY  
NUCLEOTIDE SUGAR INTERCONVERSIONS

by

PRASANTH SAMBARAJU

Major Professor: James H. Prestegard

Committee: Richard A. Dluhy  
Jeffrey L. Urbauer  
Maor Bar-Peled

Electronic Version Approved:

Maureen Grasso  
Dean of the Graduate School  
The University of Georgia  
August 2007

## DEDICATION

To my mother Sambaraju Urmila, father Sambaraju Narasimha Rao & brothers  
Srinivas and Prakash.

## ACKNOWLEDGEMENTS

I would like to thank my advisor Dr. James H. Prestegard for giving an opportunity to work in his group. His guidance, support and encouragement were helpful during this period. I would like to thank Dr. Bar-Peled and his lab members for their support in the laboratory during my research. I would also like to thank my other committee members Dr. Dluhy and Dr. Urbauer. I thank Dr. John Gluskha for helping me in using the NMR spectrometers. I also thank the all group members for their support and help. I would like to thank all my friends at UGA.

Finally I would like to thank all my family members for their unqualified support during all these years.

## TABLE OF CONTENTS

	Page
ACKNOWLEDGEMENTS .....	v
LIST OF FIGURES.....	viii
CHAPTER	
1 Introduction .....	1
1.2 References.....	3
2 Review of Literature .....	4
2.1 Golgi apparatus.....	7
2.2 Pectins .....	9
2.3 UDP-Glucuronic acid.....	13
2.4 Nucleotide Sugar Interconverting Enzymes .....	15
2.5 Statistical Total Correlation Spectroscopy.....	19
2.6 References.....	22
3 NMR detection of UDP-Apiose/xylose synthesis over a time course .....	24
3.1 Experimental .....	24
3.2 Results and Discussions .....	26
3.3 Conclusions.....	29
4 NMR methods to understand glycosylation within the Golgi .....	38
4.1 Experimental .....	38
4.2 Results and Discussions .....	42

4.3 Conclusions.....	43
APPENDICES .....	65
A Matlab code to generate Hilbert-transform matrix.....	65
B Matlab commands .....	66
C Write spec macro.....	68

## LIST OF FIGURES

	Page
Figure 2.1: Model for synthesis of Pectic polysaccharides in Golgi apparatus.....	8
Figure 2.2.1: Primary Structure of Homogalacturonan .....	11
Figure 2.2.2: Structure of RG-I .....	12
Figure 2.2.3: Partial structure of RG-II .....	14
Figure 2.4.1: Mechanism for UDP-Glc dehydrogenase .....	17
Figure 2.4.2: Mechanism for UDP-GlcA decarboxylase .....	18
Figure 2.4.3: Mechanism for UDP-Apiose/xylose synthase.....	20
Figure 3.1: SDS-PAGE after protein expression of UDP-Apiose synthase .....	30
Figure 3.2: Results from HPLC based UDP-Apiose/xylose synthase assays.....	31
Figure 3.3: NMR spectra after addition of UDP-Apiose/xylose synthase + UDP-GlcA + NAD at pH 7.8, 35 <sup>0</sup> C .....	32
Figure 3.4: NMR spectra after addition of UDP-Apiose/xylose synthase + UDP-GlcA + NAD at pH 6.5, 35 <sup>0</sup> C .....	33
Figure 3.5: UDP-Apiose and its degradation products .....	34
Figure 3.6: STOCSY spectrum from data at pH 7.8 .....	35
Figure 3.7: Correlation between UDP-Apiose and Apiofuranose-1,2-cyclic phosphate.	36
Figure 3.8: Asynchronous correlation plot.....	37
Figure 4.1: SDS-PAGE of expressed proteins .....	45
Figure 4.2: SDS-PAGE of expressed proteins .....	46

Figure 4.3: Results from HPLC based NDP-sugar pyrophosphorylase assays.....	47
Figure 4.4: Results from HPLC based UDP-Glc dehydrogenase assays.....	48
Figure 4.5: Results from HPLC based UDP-GlcA decarboxylase assays.....	49
Figure 4.6: Results from HPLC based UDP-Apiose/xylose synthase assays.....	50
Figure 4.7: Results from HPLC based UDP-GlcA epimerase assays.....	51
Figure 4.8: Results from HPLC based Galk assays.....	52
Figure 4.9: <sup>1</sup> H NMR spectrum of UDP-GlcA.....	53
Figure 4.10: <sup>1</sup> H NMR spectrum of UMP.....	54
Figure 4.11: <sup>1</sup> H NMR spectrum ~ 0 min of pea Golgi + D <sub>2</sub> O.....	55
Figure 4.12: <sup>1</sup> H NMR spectrum ~ 7 hr of pea Golgi + D <sub>2</sub> O.....	56
Figure 4.13: <sup>1</sup> H NMR spectra of pea Golgi + D <sub>2</sub> O + UDP-GlcA.....	57
Figure 4.14: <sup>1</sup> H NMR spectra with expanded region between 5.5 - 8.3 ppm.....	58
Figure 4.15: <sup>1</sup> H NMR spectra of pea Golgi + D <sub>2</sub> O + UDP-GlcA.....	59
Figure 4.16: <sup>1</sup> H NMR spectra with expanded region between 5.6 - 8.4 ppm.....	60
Figure 4.17: <sup>1</sup> H NMR spectrum of UDP-xylose.....	61
Figure 4.18: <sup>1</sup> H NMR spectrum ~ 0 min of maize Golgi + D <sub>2</sub> O.....	62
Figure 4.19: <sup>1</sup> H NMR spectrum ~ 0 min of maize Golgi + D <sub>2</sub> O + UDP-GlcA.....	63
Figure 4.20: <sup>1</sup> H NMR spectrum ~ 5 hr of maize Golgi + D <sub>2</sub> O + UDP-GlcA.....	64

## Chapter 1

### Introduction

Eukaryotic cells have a coating of complex glycans attached to proteins and lipids of the cell membrane. They can also be found in the extracellular spaces between the cells types (1), and more specialized cells secrete polymeric glycans that serve structural and other functions. The attachment of sugar residues to the proteins is one of the most complicated, nontemplated co- or post-translational modifications. Glycosylation is controlled by factors that differ among cell types and species (2). N-linked, O-linked and C-linked are three types of protein linked glycans. In plants and animals, N-glycosylation is involved in protein maturation, protein folding, stability and transport to their destination. In animals it is also involved in apoptosis and allergenic immune responses (3). In plants cell wall cellulose biosynthesis depends on N-glycosylation of enzymes like mannose-1-phosphate guanylyltransferase (4) and  $\alpha$ -Glucosidase I (5).

Glycosylation of proteins represents a highly complex series of events that involves enzymatic formation and breakdown of glycosidic linkages achieved by the action of glycosyltransferases and glycosidases (6). The enzymes involved in this process are located within the Golgi cisternae in the sequence in which they act. This compartmentalization of enzymes leads to efficient synthesis of glycoconjugates and prevents undesired competing reactions (7). The objective of this thesis is to understand the glycosylation process in cell wall polysaccharide synthesis by application of Nuclear

Magnetic Resonance (NMR) along with the use of modern statistical methods, STOCSY. This approach can be considered as an application of metabonomics which involves quantitative measurement of time-related metabolic response (8).

Metabonomic studies involve analysis of spectroscopic data of complex samples from  $^1\text{H}$  NMR spectroscopy with the help of multivariate statistical methods. This thesis involves development of NMR based methods along with multivariate statistical techniques to detect the interconversion of sugar nucleotides. Enzymes involved in the production of UDP sugars used by plants in the production of cell wall polysaccharides were selected as an initial target. In the first step, an *in vitro* NMR method was developed to detect UDP-Apiose formation from UDP-Glucuronic acid in presence of UDP-Apiose/Xylose synthase. The UDP-Apiose formed is an unstable product which degrades to apiofuranosyl-1,2-cyclic phosphate and UMP. So to confirm the formation of UDP-Apiose unambiguously, data were analyzed using STOCSY. The second step involved development of an in-organelle NMR method to understand the glycosylation process within the Golgi apparatus. Different sugar nucleotide interconverting enzymes were expressed, which in turn could be used to generate  $^{13}\text{C}$  labeled sugar nucleotides. This method would lay the ground work to study the conversion of  $^{13}\text{C}$  labeled sugar nucleotides within the Golgi using NMR.

## 1.2 References

1. Shriver, Z., Raguram, S., and Sasisekharan, R. (2004) *Nature Reviews Drug Discovery* **3**(10), 863-873
2. Spiro, R. G. (2002) *Glycobiology* **12**(4), 43R-56R
3. Joly, C., Leonard, R., Maftah, A., and Riou-Khamlichi, C. (2002) *Journal of experimental botany* **53**(373), 1429-1436
4. Lukowitz, W., Nickle, T. C., Meinke, D. W., Last, R. L., Conklin, P. L., and Somerville, C. R. (2001) *PNAS* **98**(5), 2262-2267
5. Gillmor, C. S., Poindexter, P., Lorieau, J., Palcic, M. M., and Somerville, C. (2002) *J. Cell Biol.* **156**(6), 1003-1013
6. Lairson, L. L., and Withers, S. G. (2004) *Chemical Communications* (20), 2243-2248
7. Colley, K. J. (1997) *Glycobiology* **7**(1), 1-b-13
8. Robertson, D. G. (2005) *Toxicol. Sci.* **85**(2), 809-822

## **Chapter 2**

### **Review of Literature**

The presence of plants on earth can be dated back to approximately 480 million years ago. The early plants are related to extant bryophytes, which then transformed to tracheophytes that dominate the earth surface (1). Tracheophytes are also called vascular or higher plants, which are comprised of many cells organized to maintain and control the functions and guide the development of plants.

Plant cells divide continuously throughout their lives. They can grow indefinitely and retain the quality of young plants (2). Plant cells are enclosed within a cell wall. Chemically the cell walls of higher plants are mainly composed of polysaccharides and proteins along with small amounts of lipids and ribonucleic acid (3). There are two types of cell walls, primary and secondary. The primary cell wall is deposited during the cell growth. It plays a significant role in mechanical stability and extensibility, which permits cell expansion without cell rupture. It also acts as defense against microorganisms and is involved in intercellular signaling (1). The secondary cell wall is deposited after the cessation of cell growth and confers mechanical stability. The primary and secondary cell wall contains cellulose microfibrils embedded in an amorphous substance called a matrix. Pectin and hemicellulose are the heteropolymers that are part of the matrix. The secondary cell wall in addition is imbued with lignins (4).

The middle lamella is the first wall deposited after cell division, which contains pectin. A primary cell wall is then laid to support the middle lamella. Chemically it

contains pectin, cellulose, hemicellulose and proteins. During growth, a plant cell extends many times its original length. So the cell wall has to resist the tension generated by turgor pressure. Cell growth is also accompanied by an increase in total area of the cell wall. The cell wall maintains these functions by a mixture of polysaccharides and proteins that control the assembly and extension of the cell wall. These polysaccharides are critical for deposition and further extension of the cellulosic glycan network (2).

Initially the cell wall was thought to be a dead, structureless box. The cell wall is now viewed as a highly complex structure, which is involved in performing diverse and essential functions. It can be considered as an active metabolic compartment (2). The composition of the cell wall has a role in cell growth as the polysaccharide composition changes during development. The plant cell wall polysaccharide composition is determined by many factors like environment and conditions of extraction like solvent, pH.

The cell wall of plants contains cellulose, xyloglucans, hemicellulose, pectins and proteins. Cellulose is a polymer consisting of chains of  $\beta$ -1,4-linked glucose residues. Cellulose exists as a composite of many chains called microfibrils. The polymeric chains of glucose are attached by hydrogen and Van der Waals bonds which lead to crystallization of cellulose in some parts of microfibrils. The amorphous or less crystallized regions lie in between the crystalline domains. The crystalline areas form tight arrays which protect the glycoside bonds from cell wall degrading enzymes. Cellulose and other components in the cell wall make it a very compact and inaccessible structure thereby protecting it from foreign bodies (5).

Hemicelluloses are polysaccharide molecules that provide a cross-linking matrix to the cellulose microfibrils. They can be classified into xyloglucans, mannans, glucuronoarabinoxylans and mixed linkage glycans. It is assumed that *Cellulose Synthase Like (CSL)* genes encode Golgi-localized glycan synthases which are involved in biosynthesis of hemicellulosic polysaccharides (6).

Cellulose synthase enzyme complexes are membrane bound, and are needed for cellulose biosynthesis. Cytosolic UDP-Glucose is used as a substrate for cellulose synthesis (5). Synthesis occurs via a one-step polymerization reaction that involves transfer of glycosyl residues with inversion of configuration at the anomeric carbon. Cellulose synthase can directly bind to the UDP-Glucose and initiate the synthesis without a primer (7). Cellulose microfibrils are synthesized in the plasma membrane whereas the matrix polysaccharides, hemicelluloses and pectins are synthesized in the Golgi apparatus. They are then deposited to the wall surface by vesicles (8).

Carbohydrates have important roles like energy sources and structural elements and they are responsible for a wide range of biochemical events. In order to effectuate these functions, carbohydrates undergo modifications like covalent attachment to a wide range of molecules. They are linked to sugars, proteins, DNA, lipids and secondary metabolites. Donor sugar in an activated form is transferred to the acceptor molecule. This reaction, called glycosylation, is one in which a nucleotide diphosphate sugar serves as activated sugar. The high energy phosphoglycosyl bond provides a driving force for this reaction which is catalyzed by glycosyltransferases (9).

Plant glycosyltransferases are involved in the biosynthesis of cell wall polysaccharides, addition of N-linked glycans to glycoprotein and attachment of sugars

to hormones. They are classified on the basis of the activated molecule that donates sugars, type of sugars to which they transfer and whether they form an  $\alpha$ - or  $\beta$ -glycosidic linkage. Enzymes involved in cell wall polysaccharides are located within the secretory pathway. They are type II membrane proteins that contain a single hydrophobic segment that spans the membrane and a short amino terminal portion which faces the cytosol. Biosynthesis of matrix polysaccharides can be divided into two stages, synthesis of backbone polysaccharide and addition of side chains residues catalyzed by glycosyltransferases (10).

## **2.1 Golgi apparatus**

The presence of the Golgi apparatus in cells was discovered by Camillo Golgi in 1898. The existence of the Golgi apparatus was questioned, until its presence was corroborated by using electron microscopy (11). In plant cells, the Golgi apparatus is involved in two major functions. It assembles and processes oligosaccharide side chains of glycoprotein and proteoglycans. It is also involved in synthesis of complex polysaccharides of the cell wall (12).

The Golgi apparatus consists of stacks of membrane cisternae distributed throughout the cell. The number of cisternae depends on cell type, secretory status and species. It is hypothesized that the stacks in Golgi are compartmentalized and enzymes involved in cell wall synthesis are located in cis-cisternae (13). In a cell, different organelles are distinguished from one another by their enzymatic content. The boundaries between the endoplasmic reticulum and Golgi are unclear. To maintain the integrity of Golgi, cells manage membrane trafficking to and from the ER to maintain

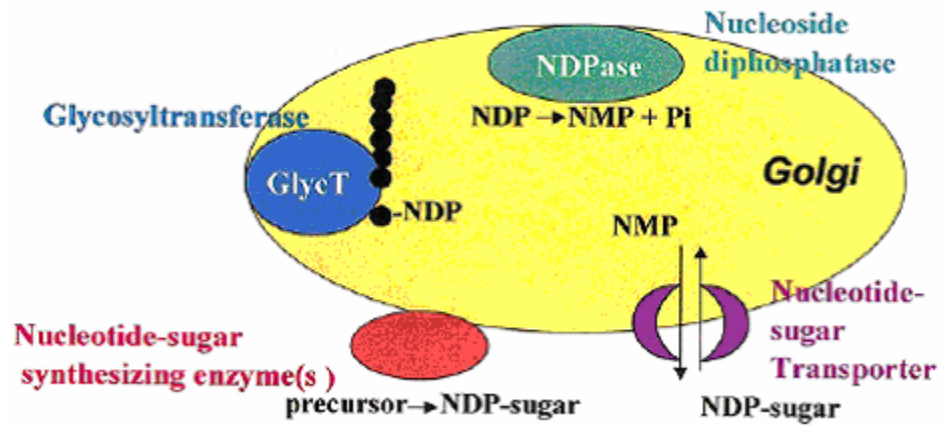


Fig. 2.1 Model for synthesis of Pectic polysaccharides in Golgi apparatus. Figure taken from (14)

secretory membrane flow through the stack. Recent studies have demonstrated that both the membranous and soluble compartments of Golgi apparatus undergo constant remodeling to preserve its structure (15).

Golgi stacks receive materials from the ER, process it and target it to the required cellular destination. They are also involved in synthesis and export of complex carbohydrates (16). The enzymes that synthesize different carbohydrate structures are localized within the membranes of Golgi. Different nucleotide diphosphate (NDP) sugars produced outside the Golgi apparatus are imported into the Golgi membrane by nucleotide sugar transporters. In the Golgi glycosyltransferases catalyze the transfer of the sugar part to the glycan. The resulting NDP is cleaved by luminal nucleotide diphosphatase (NDPase) to produce inorganic phosphate (Pi) and nucleotide monophosphate (NMP). NMP exists in antiport with the incoming NDP sugars (17).

## **2.2 Pectins**

Pectins are a group of polysaccharides that are rich in galacturonic acid (Gal A). Pectins contain distinct structural domains which undergo biosynthetic and cell wall based modifications. Linking of these polysaccharides leads to the formation of a network, which is present throughout the cell wall. It is hypothesized that it requires more than 50 glycosyltransferases for pectin biosynthesis. The three main polysaccharides present in pectin are homogalacturonan (HG), rhamnogalacturonan I (RG-I) and small amounts of rhamnogalacturonan II (RG-II). Pectin has a major role in controlling cell wall porosity, as adhesive material between cells, and is involved in deposition, slippage and extension of cellulosic-glycan network (18).

HG is a linear homopolymer of (1→4)- $\alpha$ -linked D-galacturonic acid and also

contains some GalA residues. RG-I contains a disaccharide of (1→2)- α-L-rhamnose-(1→4)- α-D-galacturonic acid. RG-II contains a (1→4)-α-linked GalA residues that is substituted by four heteropolymeric side chains (18).

HG is an abundant polysaccharide that accounts for ≈ 70% of pectin. GalA (14)substitution with xylose or apiose (19). HG has a role in cell expansion, cell development, intercellular adhesion and defense mechanism. GalA residues that are un-esterified are cross-linked by calcium forming supramolecular pectic gels. These gels are important in controlling porosity, mechanical properties of the cell wall and help in maintaining intercellular adhesion (18). The methyl-esterified HG is exported to the cell wall. Pectin methyl esterases (PMEs) present in the cell wall act on HG to de-esterify it (14) .

Pectin contains ≈ 35% of RG-I; it has a role in determining the structure and functions of the cell wall (19). It may also function as a scaffold to which other pectins like RG-II and HG are covalently attached as side chains. The ratio of GalA to rhamnose is 1:1 as an alternating sequence. It is unclear whether the GalA residues are methyl-esterified or not. RG-1 is a heavily branched structure containing neutral sugars that are attached to the C-4 of rhamnose (20).

RG-II is a complex pectic polysaccharide with a molecular weight ~5 kDa (21). RG-II is ≈ 10% of pectin (19) and is structurally unrelated to RG-I. The HG backbone in RG-II is substituted with four different oligosaccharide side chains (A, B, C & D). A, B are 2-linked whereas C, D are 3-linked to the pectic backbone. Rare sugars like D-apiose, L-aceric acid, 2-O-methyl L-fucose, 2-O-methyl D-xylose, L-galactose, 2-keto-3-deoxy-D-lyxo-heptulosaric acid and 2-keto-3-deoxy-D-*manno*-octulosonic acid are

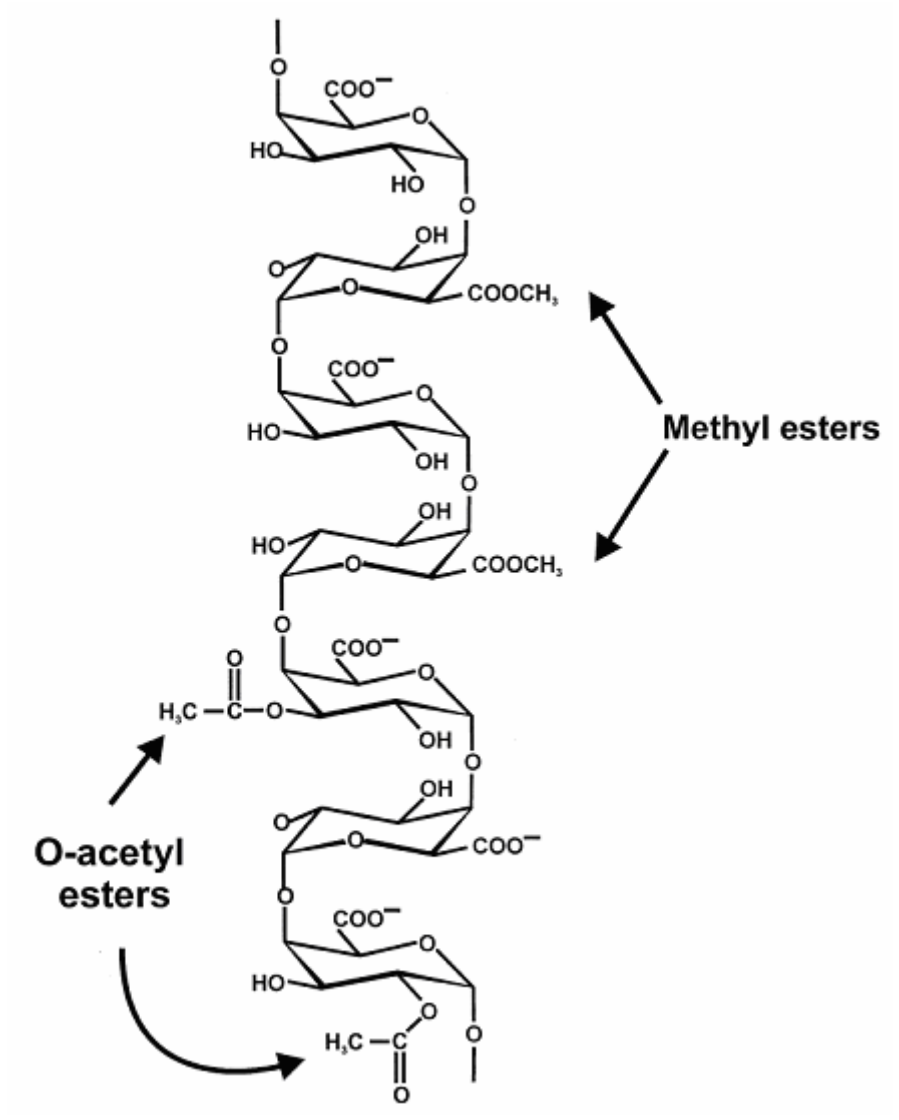


Fig. 2.2.1 Primary Structure of Homogalacturonan. Figure taken from (14)

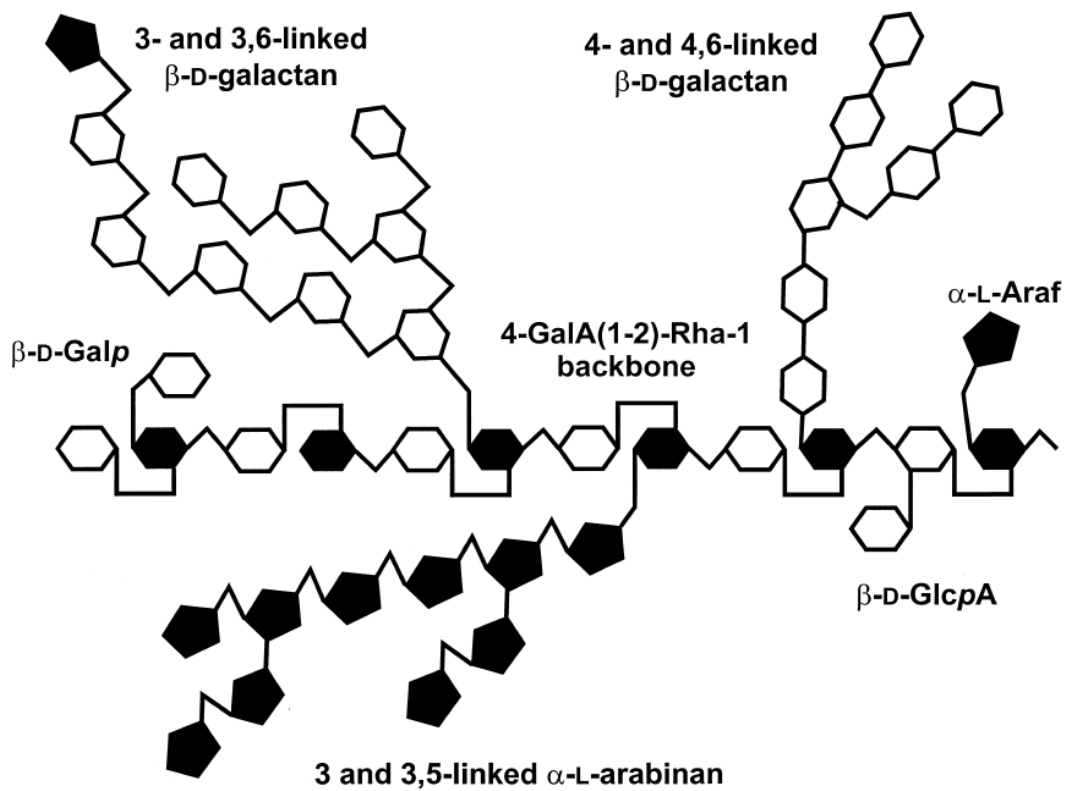


Fig. 2.2.2 Structure of RG-I showing the backbone (1 $\rightarrow$ 2)-  $\alpha$ -L-rhamnose-(1 $\rightarrow$ 4)-  $\alpha$ -D-galacturonic acid with branched sugars attached to it. Figure taken from (14)

present in RG-II (22). It contains 29 monosaccharide units which are linked by more than 12 different glycosyl linkages (21). The primary structure of RG-II has remained constant in tracheophytes. It is hypothesized that a small change in RG-II structure could reduce its ability to form borate cross-linked dimer which ultimately affects plant growth and development (1)

### **2.3 UDP-Glucuronic acid**

UDP-Glucuronic acid (UDP-GlcA) is an important intermediate in the biosynthesis of UDP-sugars like UDP-D-xylose (UDP-Xyl), UDP-arabinose (UDP-Ara), UDP-galacturonate and UDP-apiose. The UDP sugars are glycosyl donor substrates in the biosynthesis of hemicellulose and pectins. Glucuronoarabinoxylans are biosynthesized from UDP-GlcA, UDP-Ara and UDP-Xyl (23). In plants there are two pathways for UDP-GlcA biosynthesis. In the *de novo* pathway, various UDP-sugars are synthesized from UDP-Glc as substrate. Different monosaccharides released from cell-wall polysaccharides, glycoproteins and glycolipids are incorporated into the cell. These monosaccharides are then converted to UDP-sugars or GDP-sugars *via* monosaccharide 1-phosphate in the salvage pathway. The salvage pathway requires many enzymes, monosaccharide kinases and nucleotide sugar pyrophosphorylases for generation of monosaccharide 1-phosphates (24).

UDP-Glc pyrophosphorylase catalyzes conversion of  $\alpha$ -D-glucose-1-phosphate to UDP-Glc *in vivo*. In plants UDP-Glc can also be synthesized from sucrose, catalyzed by sucrose synthase. UDP-Glc is converted to UDP-Gal by epimerization catalyzed by UDP-glucose 4-epimerase. Alternatively in the salvage pathway, Gal-1-P is converted to UDP-Gal by UDP-Gal pyrophosphorylase in presence of UTP (25).



UDP-Glc dehydrogenase converts UDP-Glc to UDP-GlcA, whereas the salvage pathway uses Glc-6-P as substrate for UDP-Glc synthesis. UDP-Xyl is obtained by decarboxylation of UDP-GlcA catalyzed by UDP-GlcA decarboxylase (25). UDP-Apiose is formed from UDP-GlcA by decarboxylation followed by re-arrangement of the carbon skeleton and ring contraction. The exact mechanism of rearrangement leading to the formation of UDP-Apiose is not clear (27). UDP-xylose is also formed so the enzyme is named as UDP-D-Apiose/UDP-D-Xylose synthase. It was found that depletion of this enzyme results in RG-II deficiency leading to cell wall thickening and cell death (28).

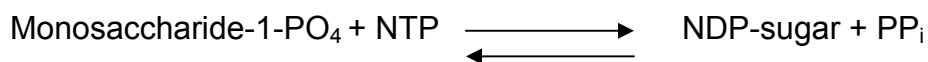
#### **2.4 Nucleotide Sugar Interconverting Enzymes**

UDP-sugars serve as substrates for synthesis of polysaccharides and glycolipids in higher plants. The following nucleotide sugar interconverting enzymes were expressed and assayed for their activity in my research work. These enzymes would be used to synthesize <sup>13</sup>C labeled nucleotide sugars which would be used study their interconversion within the Golgi apparatus.

- i) NDP Sugar Pyrophosphorylase (EC number for UDP sugar pyrophosphorylase is 2.7.7.64)
- ii) UDP-Glucose Dehydrogenase (UGD, EC number is 1.1.1.22)
- iii) UDP-Glucuronic acid Decarboxylase (UXS, EC number is 4.1.1.35)
- iv) UDP-Apiose / Xylose Synthase (EC number was not given)
- v) UDP-Glucuronic acid epimerase (EC number 5.1.3.6)

UDP-sugars are synthesized during the salvage pathway in higher plants. In the salvage pathway, free monosaccharides are released by the degradation of polysaccharides and glycoconjugates are phosphorylated by action of monosaccharide

kinases. They are converted to nucleotide sugars by action of phosphorylases in presence of their respective nucleotide triphosphates are cosubstrates. They catalyze the forward (synthesis of NDP-sugars) and reverse (pyrophosphorylisis) reaction.



NDP sugar Pyrophosphorylase catalyzes the formation of UDP-Glucose, UDP-Galactose, UDP-Glucuronic acid, UDP-L-arabinose and UDP-Xylose from their respective monosaccharide-1-phosphates in presence of UTP as co-substrate (29). UDP-Glucose is involved in biosynthesis of cell wall polysaccharides and is found in cytosol and some to extent in the amyloplast and Golgi(30).

UDP-Glucose Dehydrogenase (UGD) catalyzed  $\text{NAD}^+$  dependent oxidation of UDP-Glucose to UDP-Glucuronic acid (UDP-GlcA). The enzyme oxidizes 2-fold oxidation of alcohol to acid without releasing the aldehyde intermediate. The mechanism of action of bacterial UGD has been studied extensively (31).

UDP-Glucuronic acid decarboxylase (UXS) catalyzed the conversion of UDP-GlcA to UDP-Xylose. The mechanism for this decarboxylation reaction might involve several steps. In the first step, UDP-GlcA is oxidized to UDP-4-keto-GlcA, which undergoes decarboxylation to produce UDP-4-keto pentose. Stereospecific reduction would generate the product, UDP-Xylose (32).

UDP-Galacturonic acid (UDP-GalA) is produced by epimerization of UDP-GlcA, a reaction catalyzed by UDP-GlcA 4-epimerase. UDP-GalA serves as precursor for synthesis of various cell surface polysaccharides in plants (33). The mechanism of epimerization is assumed to be similar to the UDP-Glucose to UDP-Galactose interconversion, involving the formation of an keto-sugar intermediate (34).

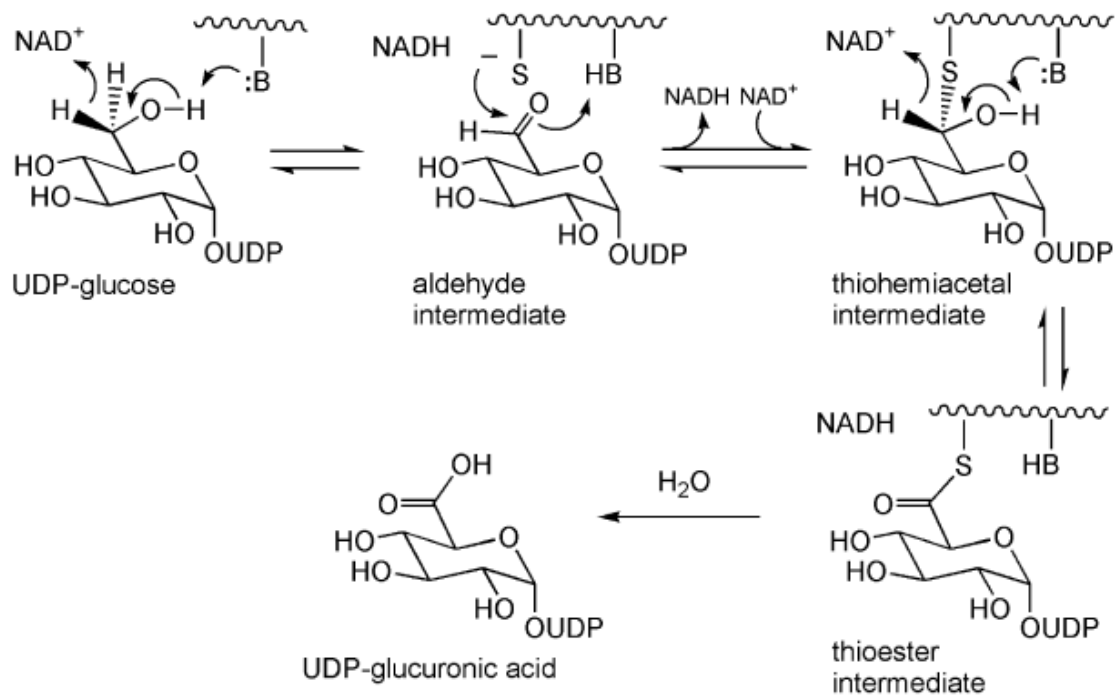


Fig.2.4.1 Mechanism of reaction catalyzed by UDP-Glc Dehydrogenase, which converts UDP-Glucose to UDP-Glucuronic acid . Figure taken from (31)

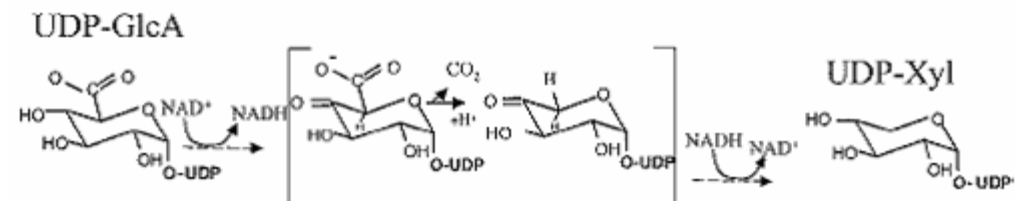


Fig.2.4.2 Proposed mechanism for UDP-GlcA decarboxylase. UDP-GlcA is converted to UDP-xylose via a 4-keto intermediate Figure taken from (35).

UDP-D-Apiose/UDP-D-Xylose synthase catalyzes the conversion of UDP-GlcA to UDP-Apiose and also UDP-Xylose. It is hypothesized that formation of UDP-Apiose might involve decarboxylation followed by rearrangement leading to ring contraction and branch formation (27).

## 2.5 Statistical Total Correlation Spectroscopy (STOCSY)

We plan to use NMR to follow nucleotide sugar conversions in this thesis. STOCSY is a method for identifying NMR peaks from the same molecule in a complex mixture. This is based on the multicollinearity of intensity variables in the  $^1\text{H}$  NMR spectra. A pseudo 2D NMR spectrum can be obtained which displays the correlation intensities among various peaks. STOCSY connectivity is not limited to the connectivities that can be observed in spin physics dependent 2D NMR techniques. Correlation can be observed between resonances with no spin-coupling connectivity between them (36). Connection between two or more molecules in the same pathway can also be established as variations in their resonance intensities will be correlated. STOCSY is based on the properties of the correlation matrix (C). The correlation matrix (C) can be computed from a set of sample spectra.

$$C = 1/(n-1) * X_1 * {}^tX_2$$

The original data may have different units and variances. Autoscaling results in scaled variables with zero mean and unit variances.  $X_1$  &  $X_2$  are the autoscaled experimental matrices of dimensions  $n \times v_1$  and  $n \times v_2$ ,  $n$  is the number of spectra and  $v_1$  &  $v_2$  are the intensities at each frequency point in spectra for each matrix. C is a matrix with dimensions  $v_1 \times v_2$ . Each value in this matrix indicates the correlation coefficient between 2 variables  $X_1$ ,  $X_2$ .

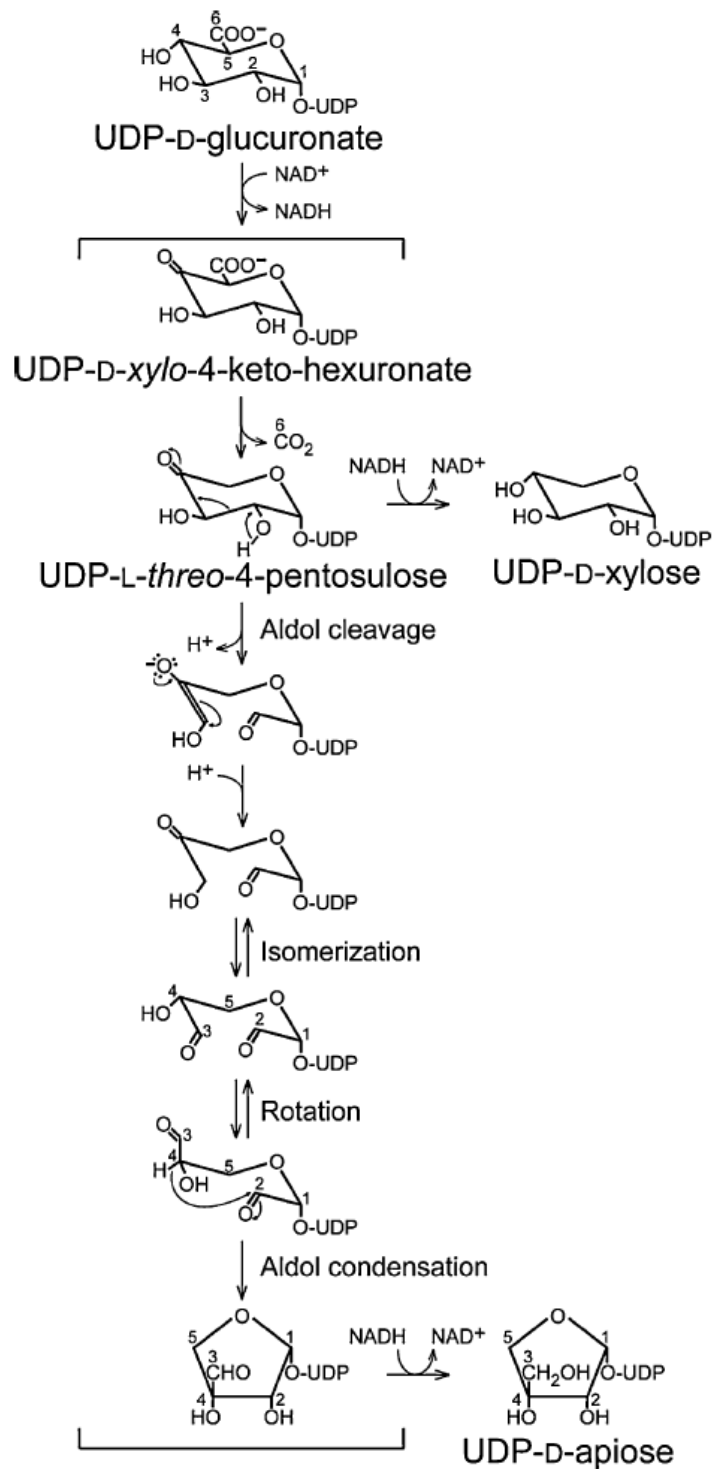


Fig. 2.4.3 Proposed mechanism for UDP-Apiose/Xylose synthase, Figure take from (27)

In identical samples, the relative intensities are totally correlated, so the correlation coefficient ( $r$ ) is 1 in all cases. This is due to the fact that the resonance intensities from a single molecule will have a fixed ratio. In samples containing a random mixture of different compounds,  $r$  will be less than 1 as spectral noise or different intensities of peaks in different spectra lead to low values. The correlation matrix for a set of spectra from samples containing different amounts of same molecule will display high correlation between resonances of the sample molecule. Two or more molecules involved in the same pathway may exhibit codependence. The correlation between different molecules in this case would be finite but could be either positive or negative depending on whether the amounts were correlated or anticorrelated. A plot of the correlation matrix yields a spectrum which is similar to that of TOCSY, 2D NMR spectra. A TOCSY spectrum is obtained through bond correlations via spin-spin coupling. Correlations are seen throughout the coupling network. A TOCSY spectrum contains diagonal and cross peaks. The diagonal peaks contain a representation of the 1D spectrum peaks whereas crosspeaks correspond to coupling through bond correlations. The resolution along the  $F_1$  domain in STOCSY is higher when compared to 2D correlation experiments. STOCSY can also be used to provide heteronuclear correlation, derive spectral splitting and J coupling. STOCSY can be considered as synchronous correlation spectrum (37).

Asynchronous correlation can be calculated by using the following relation

$$\text{Asynchronous correlation} = 1/(v-1) * X^t * H * X$$

where  $v$  corresponds to the number of points in the spectra,  $X$  is the experimental matrix and  $H$  is the Hilbert transform matrix (38).

## 2.6 References

1. Matsunaga, T., Ishii, T., Matsumoto, S., Higuchi, M., Darvill, A., Albersheim, P., and O'Neill, M. A. (2004) *Plant physiology* **134**(1), 339-351
2. Perez, S., Rodriguez-Carvajal, M. A., and Doco, T. (2003) *Biochimie* **85**(1-2), 109-121
3. Nevins, D. J., English, P. D., and Albersheim, P. (1967) *Plant physiology* **42**(7), 900-906
4. Reiter, W.-D. (2002) *Current opinion in plant biology* **5**(6), 536-542
5. Levy, I., Shani, Z., and Shoseyov, O. (2002) *Biomolecular engineering* **19**(1), 17-30
6. Lerouxel, O., Cavalier, D. M., Liepman, A. H., and Keegstra, K. (2006) *Current opinion in plant biology* **9**(6), 621-630
7. Saxena, I. M., and Brown, R. M., Jr. (2005) *Annals of botany* **96**(1), 9-21
8. Cosgrove, D. J. (2005) *Nature reviews* **6**(11), 850-861
9. Tanner, M. E. (2001) *Current Organic Chemistry* **5**(2), 169
10. Keegstra, K., and Raikhel, N. (2001) *Current opinion in plant biology* **4**(3), 219-224
11. Bentivoglio, M. (1999) *Journal of the history of the neurosciences* **8**(2), 202-208
12. Zhang, G. F., and Staehelin, L. A. (1992) *Plant physiology* **99**(3), 1070-1083
13. Wee, E. G., Sherrier, D. J., Prime, T. A., and Dupree, P. (1998) *The Plant cell* **10**(10), 1759-1768
14. Ridley, B. L., O'Neill, M. A., and Mohnen, D. (2001) *Phytochemistry* **57**(6), 929-967
15. Matheson, L. A., Hanton, S. L., and Brandizzi, F. (2006) *Current opinion in plant biology* **9**(6), 601-609
16. Hawes, C. (2005) *The New phytologist* **165**(1), 29-44
17. Handford, M., Rodriguez-Furlán, C., and Orellana, A. (2006) *Brazilian Journal of Medical and Biological Research* **39**, 1149-1158
18. Willats, W. G., McCartney, L., Mackie, W., and Knox, J. P. (2001) *Plant molecular biology* **47**(1-2), 9-27
19. Bacic, A. (2006) *Proceedings of the National Academy of Sciences of the United States of America* **103**(15), 5639-5640
20. Somerville, C., Bauer, S., Brininstool, G., Facette, M., Hamann, T., Milne, J., Osborne, E., Paredes, A., Persson, S., Raab, T., Vorwerk, S., and Youngs, H. (2004) *Science* **306**(5705), 2206-2211
21. du Penhoat, C. H., Gey, C., Pellerin, P., and Perez, S. (1999) *Journal of Biomolecular NMR* **14**(3), 253-271
22. O'Neill, M. A., Ishii, T., Albersheim, P., and Darvill, A. G. (2004) *Annual review of plant biology* **55**, 109-139
23. Karkonen, A., Murigneux, A., Martinant, J. P., Pepey, E., Tatout, C., Dudley, B. J., and Fry, S. C. (2005) *The Biochemical journal* **391**(Pt 2), 409-415
24. Kotake, T., Hojo, S., Yamaguchi, D., Aohara, T., Konishi, T., and Tsumuraya, Y. (2007) *Bioscience, biotechnology, and biochemistry* **71**(3), 761-771
25. Reiter, W.-D., and Vanzin, G. F. (2001) *Plant molecular biology* **47**(1), 95-113

26. O'Neill, M. A., Warrenfeltz, D., Kates, K., Pellerin, P., Doco, T., Darvill, A. G., and Albersheim, P. (1996) *J. Biol. Chem.* **271**(37), 22923-22930
27. Molhoj, M., Verma, R., and Reiter, W. D. (2003) *Plant J* **35**(6), 693-703
28. Ahn, J. W., Verma, R., Kim, M., Lee, J. Y., Kim, Y. K., Bang, J. W., Reiter, W. D., and Pai, H. S. (2006) *The Journal of biological chemistry* **281**(19), 13708-13716
29. Kotake, T., Yamaguchi, D., Ohzono, H., Hojo, S., Kaneko, S., Ishida, H. K., and Tsumuraya, Y. (2004) *The Journal of biological chemistry* **279**(44), 45728-45736
30. Kleczkowski, L. A., Geisler, M., Ciereszko, I., and Johansson, H. (2004) *Plant physiology* **134**(3), 912-918
31. Ge, X., Penney, L. C., van de Rijn, I., and Tanner, M. E. (2004) *European journal of biochemistry / FEBS* **271**(1), 14-22
32. Harper, A. D., and Bar-Peled, M. (2002) *Plant physiology* **130**(4), 2188-2198
33. Gu, X., and Bar-Peled, M. (2004) *Plant physiology* **136**(4), 4256-4264
34. Firdich, E., and Whitfield, C. (2005) *Journal of bacteriology* **187**(12), 4104-4115
35. Bar-Peled, M., Griffith, C. L., and Doering, T. L. (2001) *PNAS*, 211229198
36. Lindon, J. C., Holmes, E., and Nicholson, J. K. (2007) *FEBS Journal* **274**(5), 1140-1151
37. Cloarec, O., Dumas, M. E., Craig, A., Barton, R. H., Trygg, J., Hudson, J., Blancher, C., Gauguier, D., Lindon, J. C., Holmes, E., and Nicholson, J. (2005) *Anal. Chem.* **77**(5), 1282-1289
38. Sasic, S., Muszynski, A., and Ozaki, Y. (2000) *J. Phys. Chem. A* **104**(27), 6380-6387

## Chapter 3

### NMR detection of UDP-Apiose/xylose synthesis over a time course

UDP-Apiose/xylose synthase catalyzes the conversion of UDP-GlcA to UDP-Apiose and UDP-xylose. Due to the inherent instability of UDP-Apiose, its formation had not been previously established. To detect the formation of UDP-Apiose a combination analytical techniques including NMR and Anion Exchange HPLC, along with a statistical method called STOCSY, were used in this thesis.

### 3.1 Experimental

#### a) Expression, extraction and purification of UDP-Apiose/Xylose synthase

A cDNA encoding potato UDP-Apiose/xylose synthase was cloned in Bar-Peled lab, and the gene was subcloned to *E.coli* expression vector pET 24d:31.2#7. 7.5 ml of overnight *E.coli* culture cells containing the pET24d:31.2#7 vector was inoculated in 240 ml of Luria-Bertani media containing kanamycin (50 µg/ml) and chloramphenicol (30 µg/ml). Cells were grown at 37°C with shaking at 250 rpm until cell density is  $A_{600} \sim 0.6$ . Gene expression was then induced by adding 0.25 ml of 1M isopropylthio-β-galactoside. The cell expression was continued for another 4 hrs at 30°C while shaking at 250 rpm. Cells were then collected by centrifugation at 6,000 g for 10 min at 4°C. A band was detected at ~ 43 kDa in the SDS-PAGE gel, which confirmed the presence of UDP-Apiose/Xylose synthase. Cells were resuspended in 10 ml cold extraction buffer containing 20 mM Tris-HCl pH 7.6, 10 % glycerol and 1mM EDTA. After adding 5 mM DTT and 0.5 mM phenylmethylsulfonyl fluoride, cells were ruptured by sonication. Then

the lysed cells were subjected to centrifugation at 4<sup>0</sup>C for 30 min at 20,000g. 1 ml of supernatant was fractionated after injecting into an anion exchange column with buffer A (50 mM sodium phosphate at pH 7.6) at a flow rate of 1 ml/min as described by Guyett and Bar-Peled (unpublished). The column was washed with buffer A until the UV absorption, A<sub>280</sub> has stabilized. A linear salt gradient in buffer A at a flow rate of 0.5 ml/min was used to elute the protein. By observing the UV absorption at A<sub>280</sub> eluted protein were detected.

#### b) Protein identification

The cDNA clone expressing UDP-Apiose was made in Bar-Peled's lab and it contains 386 aminoacids. The calculated molecular weight this enzyme was 43.19 kDa. A band at ~43 kDa was detected in SDS-PAGE gel, which confirms the expression of this protein.

#### c) HPLC assays to determine the activity of expressed protein

HPLC assay were performed before and after fractionation of UDP-Apiose/xylose synthase, using UDP-GlcA and NAD as substrates, and these are shown in figure 3.2. The products of the reaction were separated by Anion exchange and were detected by a diode array detector at 260 nm. The peaks for substrates, UDP-GlcA and NAD eluted at 24.3 min and 7.4 minutes respectively. UDP-Apiose, the product formed in the reaction could not be detected using this detector. Peaks at 17.5 and 18.3 minutes could be due to UMP and UDP-xylose respectively. No peaks for UMP and UPD-xylose were detected when the assay was performed in absence of NAD. This demonstrates the requirement of NAD for its activity. After fractionation every alternate fraction was assayed for activity. Fractions 2, 4, 6, 8, 10 & 12 exhibited activity after fractionation.

#### d) NMR based assay

NMR assay was conducted to detect the formation of UDP-Apiose from UDP-Glucuronic acid. NMR spectra were collected using a Varian Inova 800 MHz spectrometer. The assay was carried out in 90% H<sub>2</sub>O or 80 % D<sub>2</sub>O. The NMR assay adopted from Paul Guyett and Bar-Peled (unpublished) was performed using 100  $\mu$ l purified enzyme, 20  $\mu$ l of 10 mM  $\beta$ -NAD, 20  $\mu$ l of 10 mM UDP-GlcA, 25  $\mu$ l of D<sub>2</sub>O, 235  $\mu$ l of distilled water and 100  $\mu$ l of 0.5 M Phosphate buffer at different pH (6.5 and 7.8) was added to make the final volume to 500  $\mu$ l. The entire reaction was immediately transferred to an NMR tube and analyzed. A blank with no enzyme was used for shimming purposes. An NMR presaturation pulse sequence technique was used to suppress the solvent signal in the spectrum and 1D spectra were then collected. The 2D NMR technique, COSY was used for peak assignment.

### 3.2 Results and Discussion

NMR analysis of the reaction at pH 7.8 in 80% D<sub>2</sub>O at 35<sup>0</sup>C is shown in figure 3.3. The assay was carried out at pH 7.8 to mimic the pH inside a plant cell. Spectra are plotted at 25 minute intervals starting from ~15 to 490 minutes. The bottom spectrum corresponds to the initial time, which shows small signals labeled A1 to A4. The triplet at  $\delta$ 5.75 is assigned to the proton with the 1-phosphate linkage in the apiose ring and having a H1-H2 coupling of 4.5 Hz and H1-P coupling of 5.6 Hz. The resonance at 4.0 ppm is assigned to H2, based on a crosspeak in COSY (data not shown). The UDP-Apiose formed has not degraded at this point, the peaks at  $\delta$ 3.64 and  $\delta$ 4.05 are assigned to H3 and H4 of UDP-Apiose respectively. They correspond to the initial products of the reaction. These signals grow with time and decay with time. By

comparing the bottom spectrum with top spectra confirms the complete conversion of UDP-GlcA (labeled G1 to G5) to UDP-xylose (peaks labeled x1 to x5) and D-apiofuranosyl-1,2-cyclic phosphate (cA1, cA3 and cA4). They were assigned based on comparison to authentic samples obtained by Paul Guyett (data not shown). The signals labeled U5 belong to the two H-5 of ribose in UMP, which is a degradation product from UDP-Apiose. UDP-4-keto-xylose, a proposed intermediate in the reaction could be detected under these conditions. It was reported that the rate of decomposition of UDP-Apiose is slower at neutral or slightly acidic pH, the assay was repeated at pH 6.5 although the enzyme is less active.

NMR analysis of reaction at pH 6.5 in 80% D<sub>2</sub>O buffer at 35<sup>0</sup>C is shown in figure 3.4. Spectra are plotted at 50 minute intervals from the start of the reaction up to 18 hrs. The rate of the enzyme reaction was reduced at lower pH leading to accumulation of UDP-Apiose before its degradation. The peaks are labeled as UDP-Apiose (A), D-apiofuranosyl-1,2-cyclic phosphate (cA), UDP-Xylose (X) and UDP-4-keto-xylose (K). UDP-Apiose remained relatively stable up to 15 hrs under the lower pH with lower degradation. Accumulation of UDP-4-keto-Xylose was observed as well under the assay conditions. Peaks at 5.65 ppm (H1), 3.61 ppm (H2), 3.85 ppm (H3) and 3.96 & 3.59 ppm (two protons at H5) were assigned to this molecule.

The analysis of different rates of change in concentration of each component in a mixture can be achieved by constructing a correlation matrix of the spectra. So to validate the formation of UDP-Apiose, STOCSY was used. The spectrum at different time points was converted to an ASCII file using write spec macro which is part of the

Varian software for processing NMR data. Then the data were processed using MATLAB software. The correlation matrix was then obtained for the above data.

$$C(\text{correlation matrix}) = 1/(n-1) * X * X^t$$

n is the number of the spectra, X is the matrix obtained after conversion of different spectra into an ASCII file & X<sup>t</sup> is the transpose of this matrix. The contour plot of this correlation matrix results in a STOCSY spectrum which is shown in figure 3.6. STOCSY can be considered as a synchronous correlation 2D NMR plot. The synchronous correlation spectrum is characterized by the presence of peaks or autopeaks and cross peaks or off diagonal peaks. Peaks are present along the diagonal line and they always have a positive sign. The cross peaks can be either positive or negative. Correlated peaks have positive cross peaks whereas anticorrelated peaks have negative cross peaks. The correlation matrix was subjected to singular value decomposition. By plotting the eigen vector corresponding to the second highest eigen value gives the correlation between apiose and Apiofuranose-1,2-cyclic phosphate and is shown in figure 3.7. The analysis of this figure confirms that the peaks labeled A1-A4 follow the same kinetics and are strongly correlated. So these peaks must belong to the same molecule.

Asynchronous correlation was also obtained for the above data. A contour plot of asynchronous correlation results in asynchronous correlation 2D NMR plot which is shown in figure 3.8. Plot of eigen values of this matrix did not yield any correlation (data not shown).

$$\text{Asynchronous correlation} = 1/(v-1) * X^t * H * X$$

### 3.3 Conclusions

STOCSY provided the correlation between UDP-Apiose and Apiofuranose-1,2-cyclic phosphate. This would suggest that UDP-Apiose would decompose to generate the Apiofuranose-1,2-cyclic phosphate and UMP.

NMR analysis suggests that at pH 7.8 and 35<sup>0</sup>C, UDP-Apiose is produced first and in higher amounts compared to UDP-xylose. The current proposed reaction mechanism for production of UDP-apiose requires ring opening, contraction and closing followed by reduction at C-3. The production of UDP-apiose despite the fact that reduction of UDP-4-keto-xylose intermediate is energetically favored might indicate that formation of UDP-xylose could be an artifact observed under these assay conditions. Carrying out the assay *in vivo* within the Golgi could provide further evidence regarding UDP-xylose production. This might enable in understanding whether UDP-Apiose/xylose synthase produces one or two products within the Golgi.

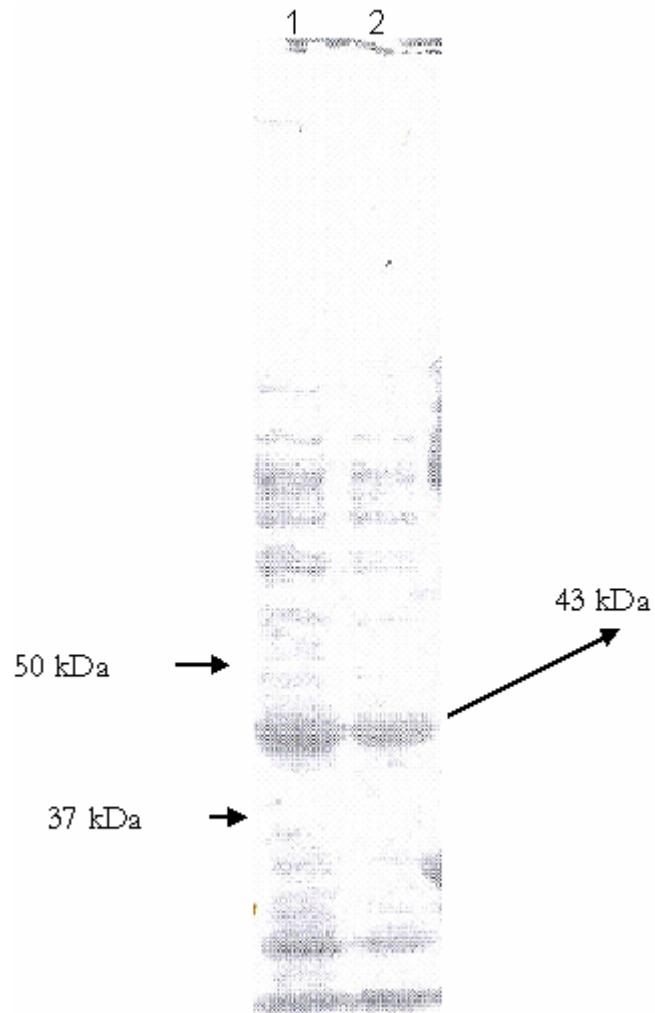
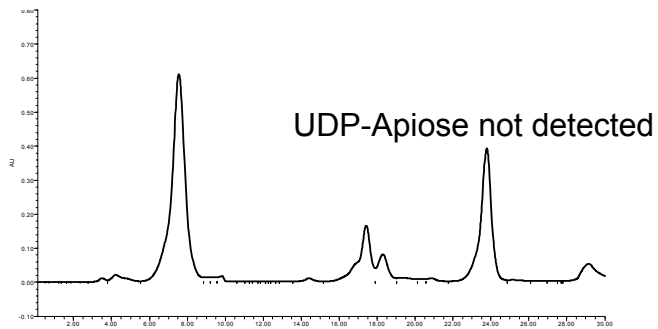


Fig.3.1 SDS-PAGE after expression of UDP-Apiose synthase with a band at 43 kDa. Lanes 1, 2 correspond to the S20 fractions. Bands corresponding to the marker lane at 37 and 50 kDa are also shown.

a) UDP-GlcA + NAD + UDP-Apiose synthase



b) UDP-GlcA + UDP-Apiose synthase

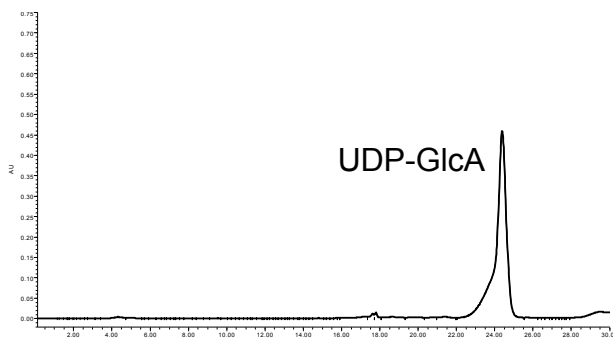


Fig.3.2 Results from HPLC based UDP-Apiose/Xylose synthase assays before fractionation of UDP-Apiose synthase. The assays were also repeated after fractionation (data not shown). (a) UDP-Apiose is formed but could not be detected. (b) In absence of NAD no UDP-Apiose is formed. These assays demonstrate the importance of NAD for enzyme activity

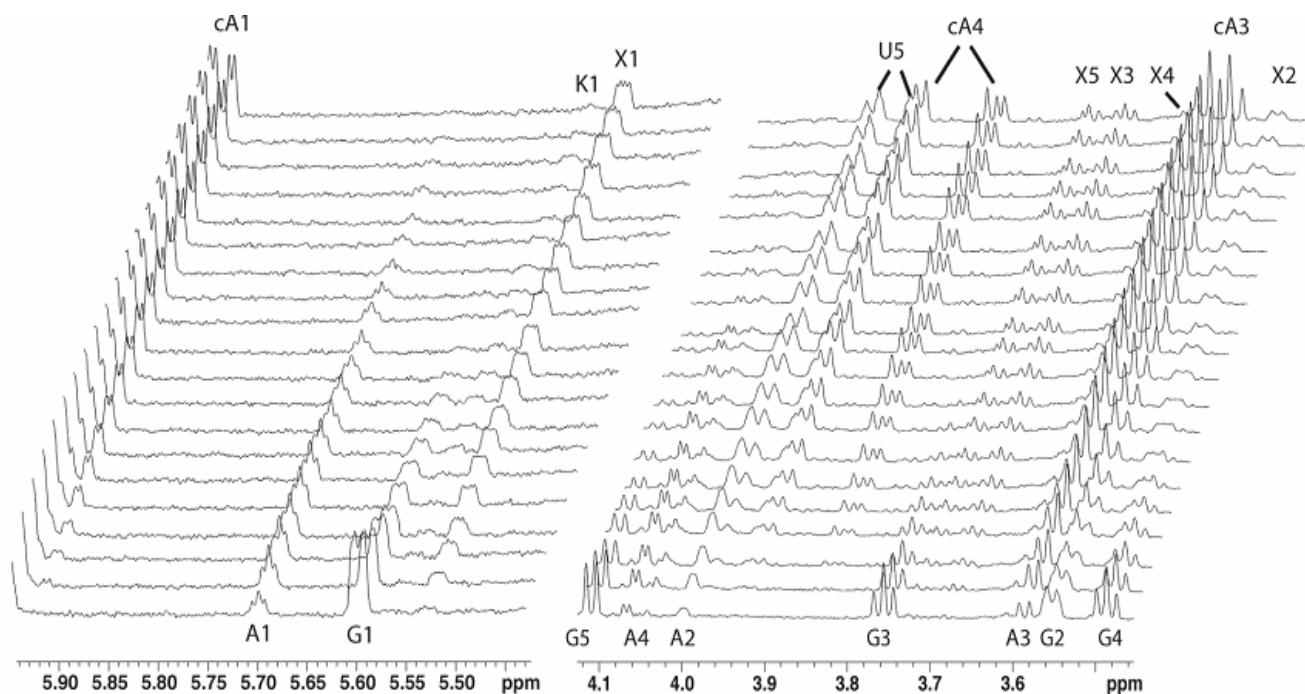


Fig.3.3: NMR spectra taken after addition of UDP-Apiose/Xylose Synthase + UDP-GlcA + NAD at pH 7.8, 35<sup>0</sup>C for 8hrs. The formation of UDP-Apiose and its decomposition can be observed in these spectra. Spectra were collected by Dr. John Glushka after assays were conducted by Paul Guyette of Bar-Peled's lab

A1, A2, A3, A4: Peak due to protons from UDP-Apiose, cA1, cA3, cA4: Peak from protons in Apiofuranose-1,2-cyclic phosphate, X1, X2, X3, X4, X5: UDP-Xylose peaks  
 U5: UMP, K1: UDP-4-keto-xylose

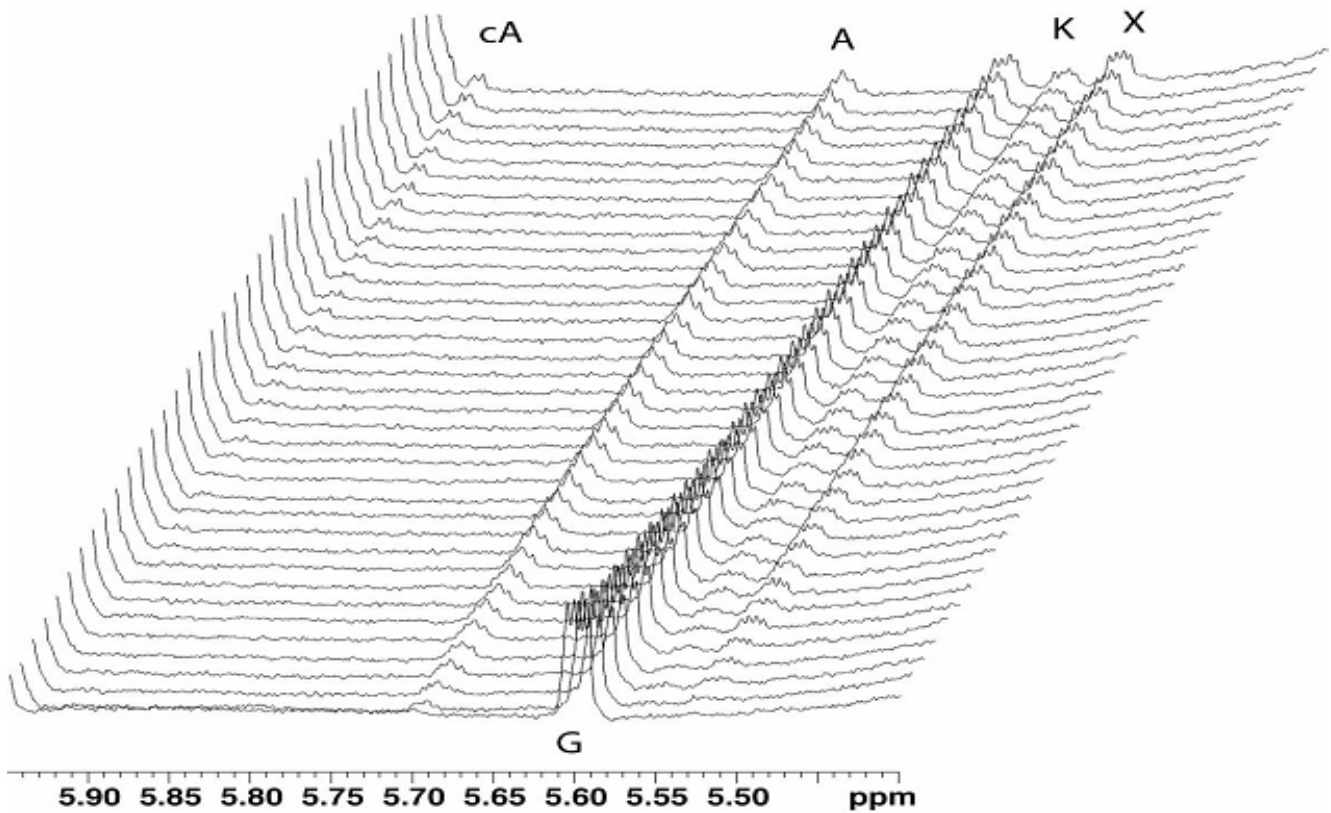
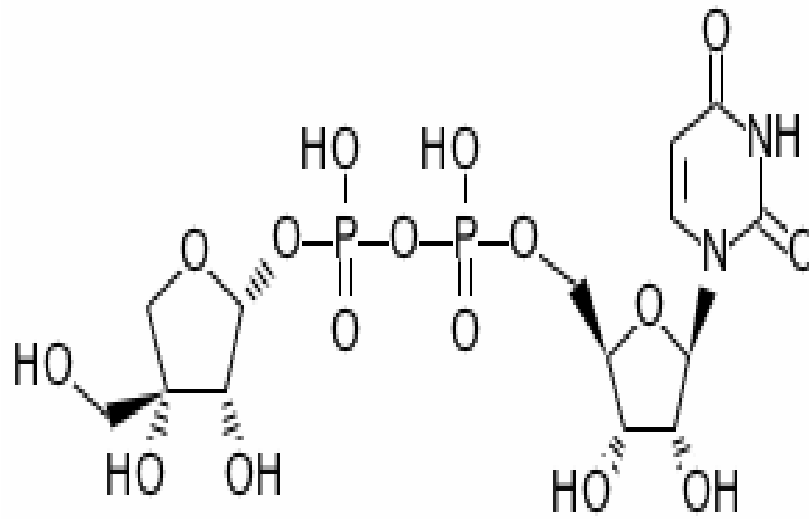
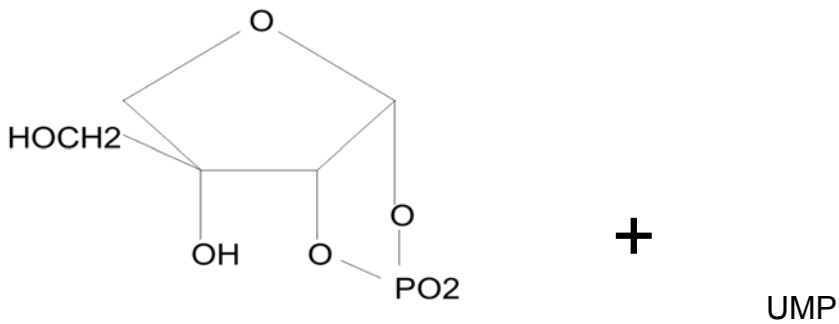


Fig.3.4: NMR spectra taken after addition UDP-Apiose/Xylose Synthase + UDP-GlcA + NAD at pH 6.5, 35°C for 18hrs. UDP-Apiose formed is relatively more stable under these assay conditions. The formation of UDP-Apiose and its decomposition can be observed in these spectra. Spectra were collected by Dr. John Glushka after assays were conducted by Paul Guyett of Bar-Peled's lab  
A: UDP-Apiose, cA: Apiofuranose-1,2-cyclic phosphate, X: UDP-Xylose, K: UDP-4-ketoxylose



UDP-Apiose



Apiofuranose-1,2- cyclic phosphate

Fig.3.5 UDP-Apiose and its degradation products

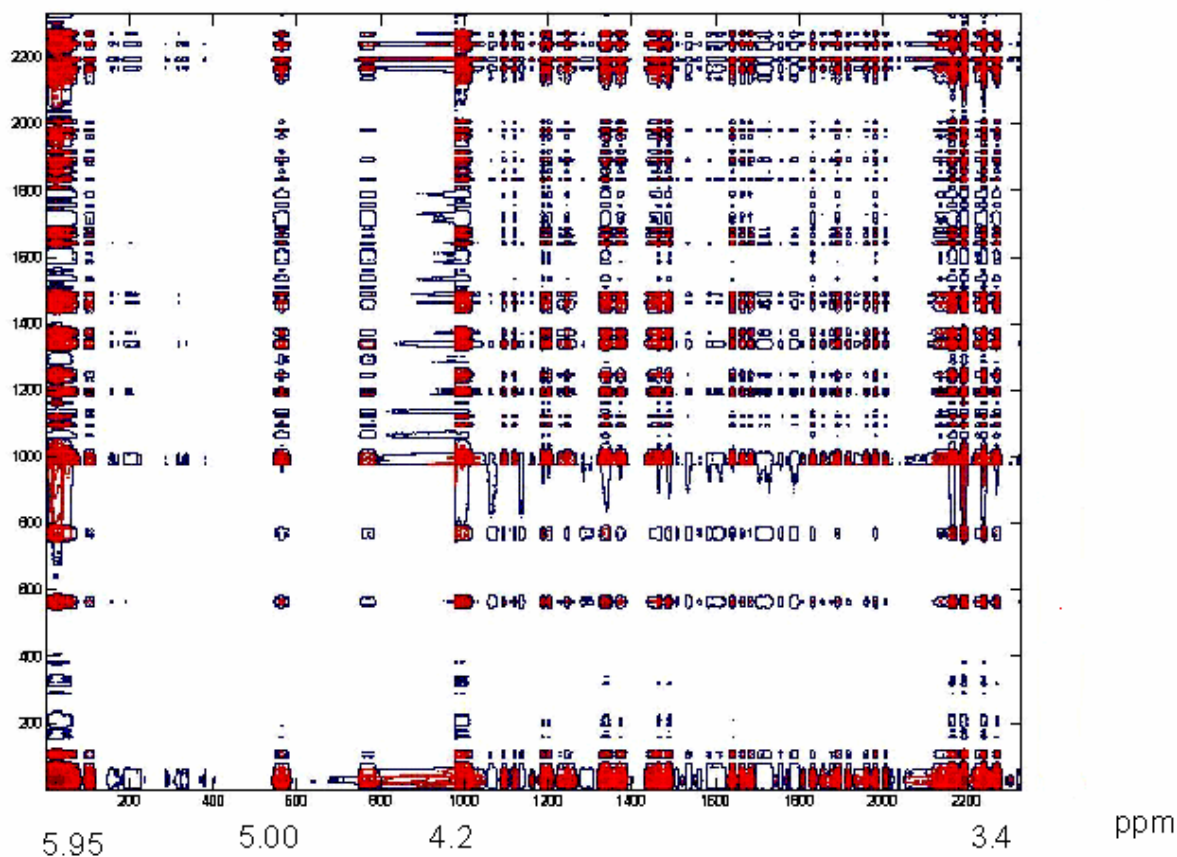


Fig.3.6 Plot of STOCSY spectrum from assay data at pH 7.8. STOCSY can be considered as synchronous correlation spectrum. Red colored spots are correlated to each other whereas colorless spots are correlated to each other.

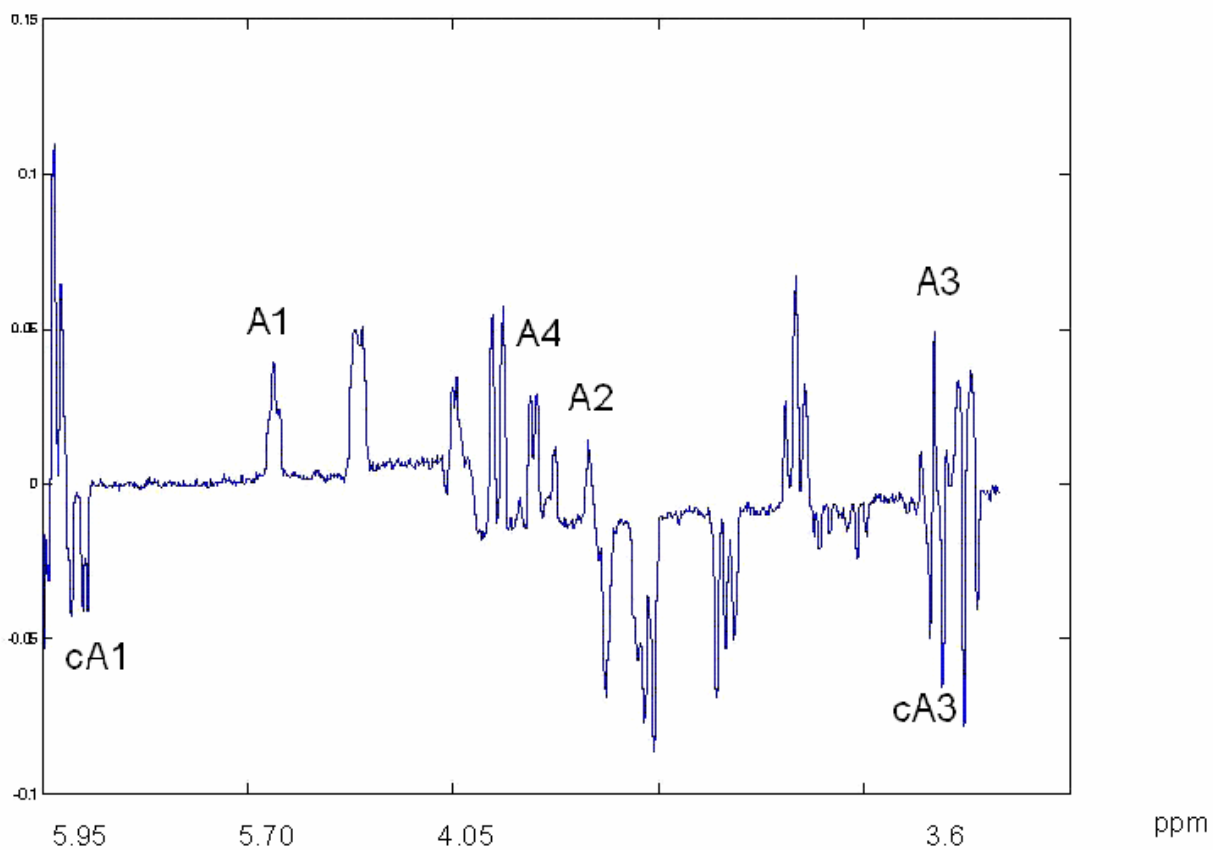


Fig.3.7 Plot of second highest eigen vector after singular value decomposition of the correlation matrix showing the correlation between UDP-Apiose (A1,A3) and Apiofuranose-1,2-cyclic phosphate (cA1, cA3) peaks.

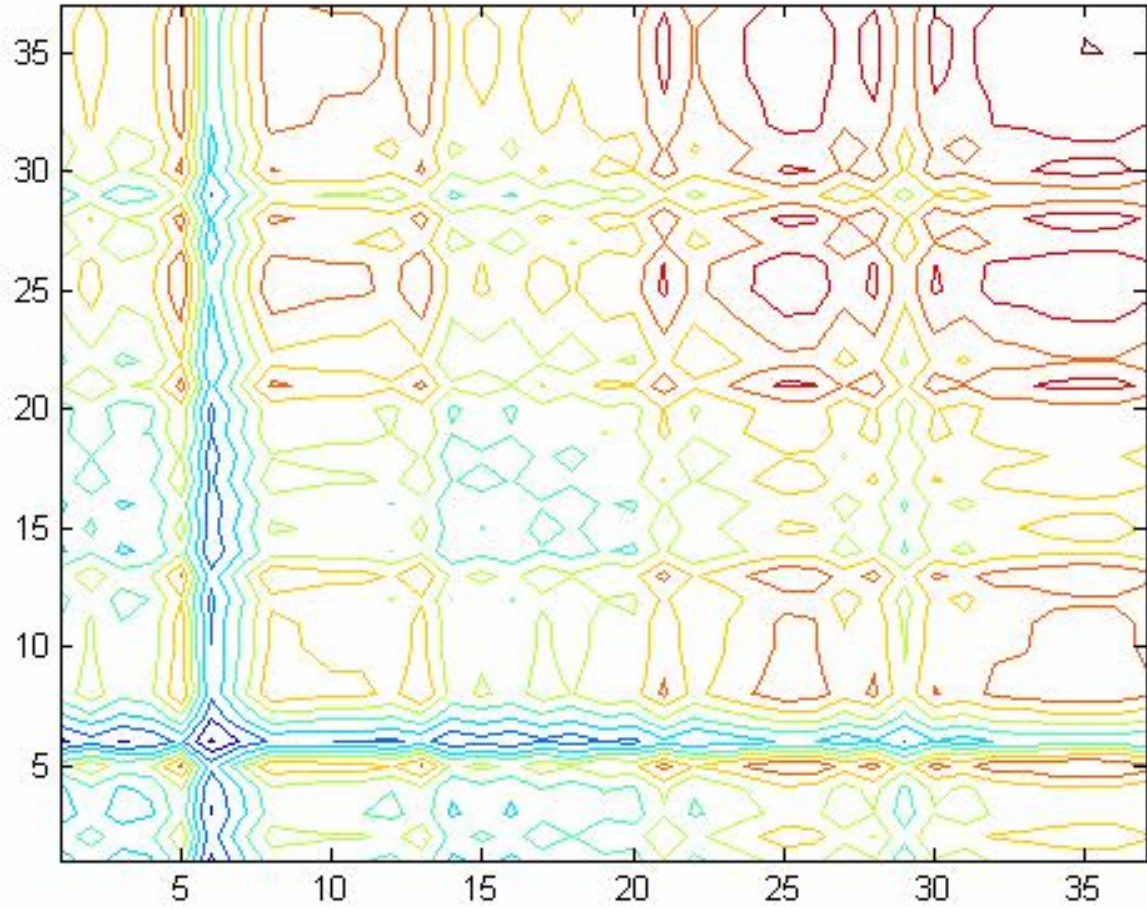


Fig.3.8: Asynchronous correlation plot obtained from the relation  $1/(v-1) * X^t * H * X$

## Chapter 4

### NMR methods to understand glycosylation within the Golgi

In higher plants the primary cell wall matrix consists of D-galacturonic acid residues in the backbone of pectic polysaccharides. UDP-sugar pyrophosphorylase converts glucose-1-phosphate to UDP-glucose in presence of UTP. UDP-glucose dehydrogenase catalyzes the irreversible conversion of UDP-glucose to UDP-Glucuronic acid. This is an important reaction as UDP-Glucuronic acid serves as precursor for biosynthesis of several pectic monosaccharides. In the plant cell, biosynthesis of cell wall polysaccharides occurs within the Golgi. By using various nucleotide sugar interconverting enzymes different UDP sugars could be generated. The aim of this study would be to add various UDP sugars to the isolated Golgi fractions and using NMR study the glycosylation process.

#### 4.1 Experimental

a) Expression, extraction and purification of Nucleotide sugar interconverting enzymes

7.5 ml of overnight *E.coli* culture cells containing pET24d:11.1#2, pET24d:101.3#1, pET24d:31.2#7, pET28b:122.2#3 and phb3-uni51:u09202 vectors from Dr. Bar-Peled lab were inoculated separately in 240 ml of Luria-Bertani media containing kanamycin and chloramphenicol. Cells were grown at 37<sup>0</sup>C with shaking at 250 rpm until cell density reached  $A_{600} \sim 0.6$ . Gene expression was then induced by adding 0.25 ml of 1M isopropylthio- $\beta$ -galactoside. The cell expression was continued for another 18 hrs at 30<sup>0</sup>C while shaking at 250 rpm. Cells were then collected by

centrifugation at 6,000 g for 10 min at 4<sup>0</sup>C. Bands characteristic for each of these proteins were detected in SDS-PAGE gel and are shown in figures 1 and figure 2. Cells were resuspended in 10 ml cold extraction buffer containing 20 mM Tris-HCl pH 7.6, 10 % glycerol and 1mM EDTA. After adding an appropriate amount of DTT and phenylmethylsulfonyl fluoride, cells were ruptured by sonication. Then the lysed cells were subjected to centrifugation at 4<sup>0</sup>C for 30 min at 20,000g. 1 ml of supernatant was fractionated after injecting into an anion exchange column with buffer A (50 mM sodium phosphate at pH 7.6) at a flow rate of 1 ml/min. The column was washed with buffer A until the UV absorption, A<sub>280</sub> had stabilized. A linear salt gradient in buffer A at a flow rate of 0.5 ml/min was used to elute the protein. By observing the UV absorption at A<sub>280</sub> eluted proteins were detected.

#### b) HPLC assays to determine activity of expressed proteins

HPLC assays were performed before and after fractionation using specific substrates for each protein. The products of the reaction were separated by Anion exchange chromatography and were detected by diode array detector at 260 nm.

- i) NDP-sugar pyrophosphorylase: The assay developed by Liron Bar-Peled (Honor's Thesis 2005) was performed by using crude protein with UTP and Glc-1-PO<sub>4</sub> as substrates and is shown in figure 4.3. The peak for UTP can be found at 24.5 min whereas peak for the product, UDP-Glc elute at 17.5 min. Flow through, fractions 8, 10, 12, 14, 16 and 18 were active after fractionation (data not shown).
- ii) UDP-Glucose dehydrogenase: The assay developed by Bar-Peled *et al* (PNAS 2001) was performed by using crude protein with UDP-Glc and NAD

- as substrates and is shown in figure 4.4. Peaks for substrates, UDP-Glc and NAD eluted at 16.5 min and 6.1 min respectively. UDP-GlcA, product eluted at 23.9 min. When the assay was performed in absence of NAD, UDP-GlcA was not formed. Fractionation led to loss of enzymatic activity (data not shown).
- iii) UDP-Glucuronic acid decarboxylase: The assay developed by Harper *et al* (Plant Physiol. 2002) was performed by using crude protein with UDP-GlcA and NAD as substrates and is shown in figure 4.5. Peaks for substrates, UDP-GlcA and NAD eluted at 23.6 min and 7.5 min respectively. UDP-xylose, product eluted at 17.2 min. UDP-xylose formation can be observed even in absence of NAD. Flow through, fractions 8 and 10 were more active whereas fractions 14 and 16 are less active after fractionation.
- iv) UDP-Apiose/xylose synthase: The assay developed by Paul Guyett and Bar-Peled (unpublished) was performed by using crude protein with UDP-GlcA and NAD as substrates and is shown in figure 4.6. Peaks for substrates, UDP-GlcA and NAD eluted at 24.3 min and 7.3 min respectively. UDP-Apiose, the product formed could not be detected. Peaks at 19.5 min and 21.0 min are ascribed to UMP and UDP-xylose respectively. When the assay was repeated in absence of NAD, where no peaks for UMP and UDP-xylose were detected. So NAD is required for the activity of this enzyme. Fractions 2, 4, 6, 8, 10 and 12 were active after fractionation (data not shown).
- v) UDP-GlcA epimerase: The assay developed by Gu *et al* (Plant Physiol. 2004) was performed by using crude protein with UDP-GlcA and NAD as substrates

and is shown in figure 4.7. Peaks for substrates, UDP-GlcA and NAD eluted at 24.3 min and 8.1 min respectively. UDP-GalA, the product is detected at 22.9 min. When the assay repeated in the absence of NAD, UDP-GalA formation could be observed. Flow through was active whereas fraction 36 displayed partial activity after fractionation (data not shown).

- vi) Galactokinase (Galk): The assay developed by P. Gleason and M. Bar-Peled (unpublished data) was performed by using crude protein with ATP and galactose as substrates, which was detected at 25.7 min and is shown in figure 4.8. The uv detector could not detect the product, Gal-1-PO<sub>4</sub>.

#### c) Isolation of Golgi

Golgi from pea and maize were isolated to study the glycosylation process within the Golgi using modified protocol (Patthil and Bar-Peled, 2003). ~90 ml of dry pea seeds (*pisum sativum*) were soaked in 1 liter of water and aerated for ~ 20 hrs. The germinated seeds are grown in moist vermiculite under dark conditions at 25<sup>0</sup>C. Golgi were extracted from a 1 – 2 cms segment of the third internode below the apical hook harvested after ~ 7 to 8 days growth.

~ 20 ml of dry maize seeds were soaked in water for overnight. The seeds were germinated and grown in moist paper under dark conditions at 25<sup>0</sup>C. Golgi was isolated by using 0.5 cms of root tip after ~ 7 to 8 days.

To the above isolated tissues from pea and maize separately, spoon-full of sand was added. The tissues were then ground in a mortar and 15 ml of cold sucrose extraction buffer was added. Then 15 µl of 1 M DTT, 15 µl of 0.1 M PMSF were added and ground until a homogenous solution was obtained. It was then poured over 2X two

layers of miracloth filter and the filtrate was collected in a centrifuge tube. It was then centrifuged at 6,000 g for 15 min at 4<sup>0</sup>C. The top layer was separated and it was then subjected to ultracentrifugation at 35,000 g for 1 hr at 4<sup>0</sup>C. The top layer was then again separated and using an aspirator the remaining liquid was removed. The solid pellet left was rinsed twice with double distilled water and aspirated to remove the water. Golgi are present in this solid pellet and sorbitol buffer and 1 µl of 1M DTT was added before the assay.

d) NMR assays to study the biotransformation of UDP-GlcA within the Golgi

Golgi obtained from the above procedure was divided into 2 fractions, each containing 285 µl of Golgi preparation. To one fraction 15 µl D<sub>2</sub>O was added and to the other fraction 15 µl of D<sub>2</sub>O and 30 µl of 20 mM UDP-GlcA dissolved in D<sub>2</sub>O was added. These fractions were transferred to 4 mm NMR tube and observed over a period of time. 600 MHz Varian NMR spectrometer was used to collect the data

## **4.2 Results and Discussions**

The expression of different nucleotide sugar interconverting enzymes was confirmed by HPLC assays. These enzymes exhibited the desired activity and could be used to generate various <sup>13</sup>C labeled UDP sugars using <sup>13</sup>C labeled precursors. Adding <sup>13</sup>C labeled UDP-sugars to isolated Golgi and monitoring the reaction using NMR might provide some insights which would be useful in understanding the glycosylation process. A preliminary study of glycosylation reaction using <sup>1</sup>H NMR was done to monitor reaction in isolated Golgi by adding UDP-GlcA to it. NMR data of the starting material, UDP-Glucuronic acid is shown in figure 4.9. It has been postulated that after transport of nucleotide diphosphate sugars into the Golgi, the sugar part is attached to

the glycan and nucleotide diphosphate is cleaved to produce inorganic phosphate and nucleotide monophosphate. NMR data showing uridine monophosphate is shown in figure 4.10. By comparing the NMR spectra of pea Golgi with pea Golgi containing UDP-GlcA in figures 4.11, 4.12, 4.13, 4.14, 4.15 & 4.16 the generation of new products can be observed. The peak at 5.65 ppm can be attributed to xylose and a reference spectrum for UDP-xylose is shown in figure 4.17 suggesting the formation of UDP-xylose. In figures 14 & 16 the H-1 resonance of xylose is labeled as X1. The intensity of this peak increases with time. Due to the presence of a huge water peak most of the pertinent information could not be obtained. By synthesizing the various  $^{13}\text{C}$  nucleotide labeled sugar, more information regarding the incorporation of these UDP sugars to glycans could be obtained. This might even enable the identification of intermediates involved in this process. So use of  $^{13}\text{C}$  labeled substrates might provide additional information which could be helpful in understanding the glycosylation process within the Golgi.

### **4.3 Conclusions**

Xyloglucans are the main hemicellulosic component in the primary cell wall of pea. Xyloglucans are synthesized and secreted entirely by the Golgi apparatus. Xylose is part of the xyloglucans and its formation could be observed from the NMR data (figures 14 and 16). NMR data has provided insight into the changes which occur within the Golgi. By using the NMR data along with the multivariate statistical methods introduced in this thesis correlation of molecular changes within the Golgi might be achieved. This would serve as groundwork for the long term goal of the project which

involves the generation of  $^{13}\text{C}$  labeled sugars and monitoring their interconversions within the Golgi apparatus.

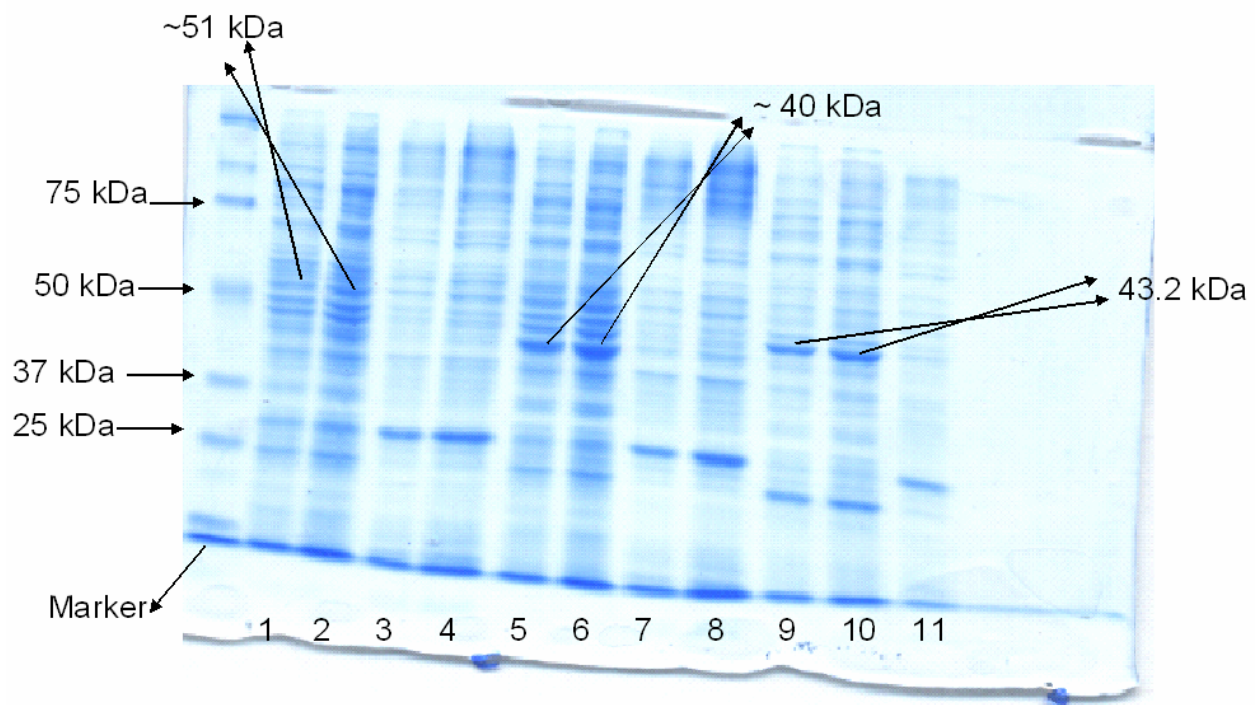


Fig.4.1 SDS-PAGE of expressed proteins. Band at ~ 51 kDa (UDP-Glucose dehydrogenase), ~ 40 kDa (UDP-Glucuronic acid decarboxylase), C ~ 43 kDa (UDP-Apiose synthase), Lanes 1, 2 correspond to S20 of UDP-Glucose dehydrogenase whereas 3 & 4 correspond to its P20 fraction. Lanes 5 and 6 correspond to S20 of UDP-Glucuronic acid decarboxylase whereas 7 & 8 correspond to its P20 fraction. Lanes 9, 10 correspond to S20 of UDP-Apiose synthase whereas lane 11 correspond to its P20.

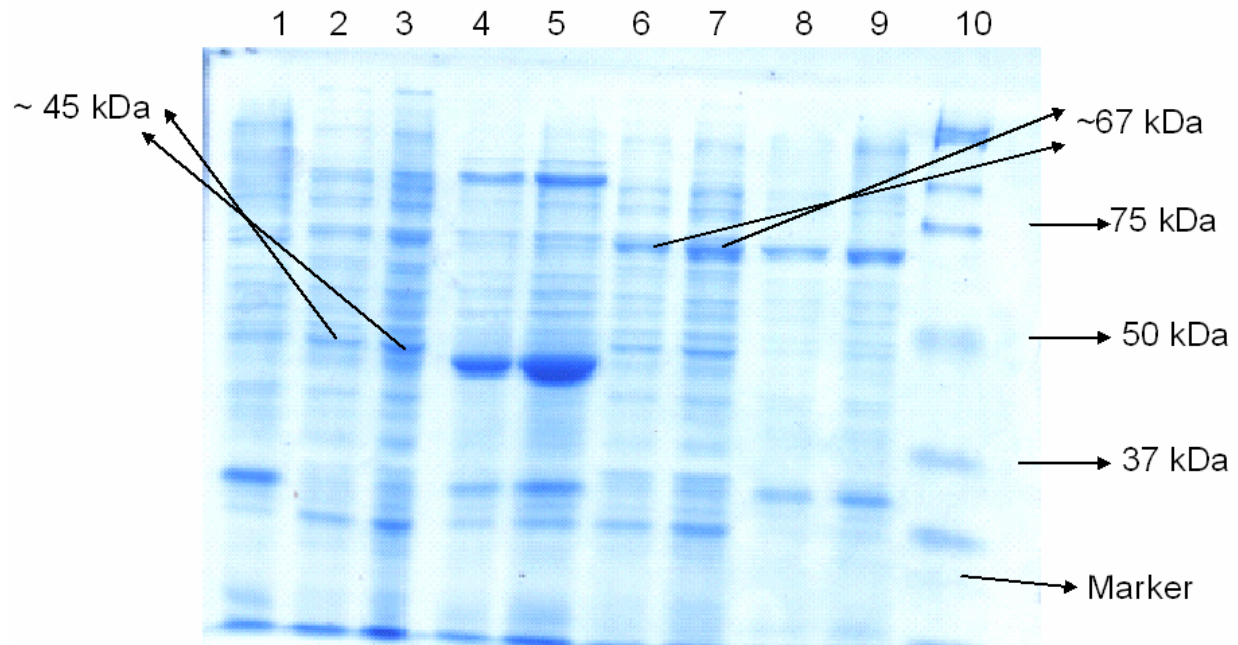
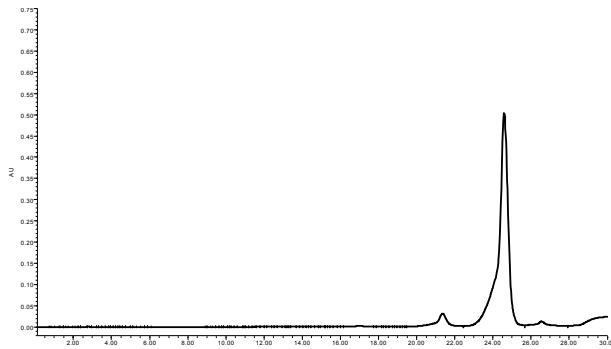


Fig.4.2 SDS-PAGE of expressed proteins, band at ~ 45 kDa (UDP-Glucuronic acid epimerase) ~ 67 kDa (NDP-pyrophosphorylase), 10 is marker lane. Lanes 2, 3 correspond to S20 of UDP-Glucuronic acid epimerase whereas 4 & 5 correspond to its P20. Lanes 6, 7 correspond to S20 of NDP-pyrophosphorylase whereas 8 & 9 correspond to its P20.

a) Standard UTP



b) UTP + NDP-sugar pyrophosphorylase + Glc-1-phosphate

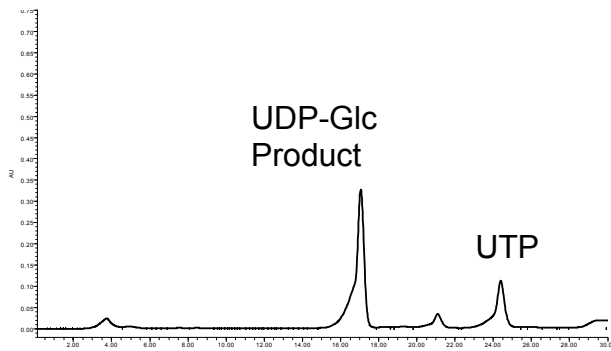
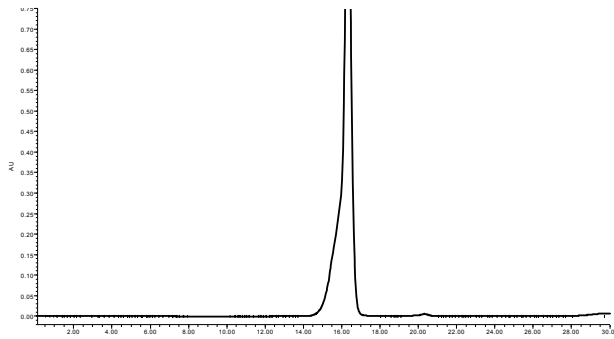
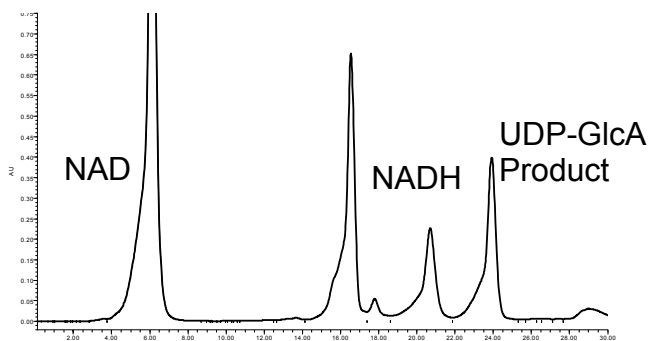


Fig.4.3: Results from HPLC based NDP-sugar pyrophosphorylase assays before fractionation. (a) UTP alone was eluted (b) Assay in presence of UTP, NDP-sugar pyrophosphorylase and Glc1-PO<sub>4</sub>. The assay was repeated after fractionation (data not shown).

a) Standard UDP-Glc



b) UDP-Glc + UGD + NAD



c) UDP-Glc + UGD

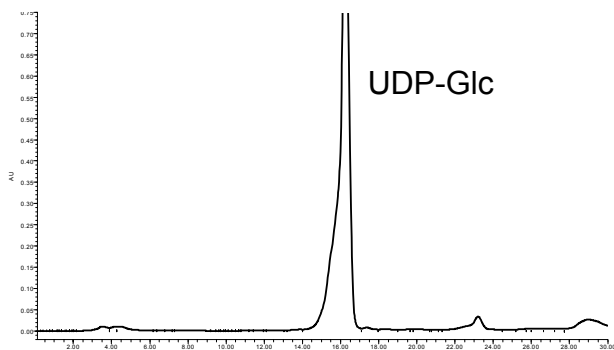
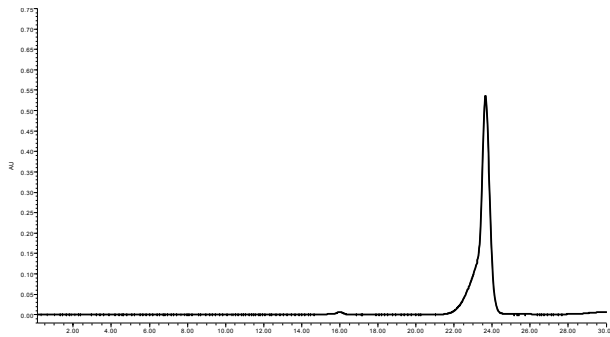
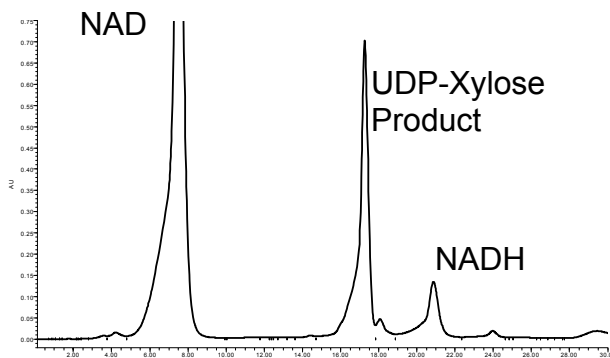


Fig.4.4: Results for HPLC based assays on UDP-Glc dehydrogenase (UGD) before fractionation. (a) UDP-Glc standard (b) assay in presence of NAD, UGD & UDP-Glc (c) assay in presence of UGD & UDP-Glc only. So NAD is required for the activity of UGD. The assays were repeated after fractionation (data not shown).

a) Standard UDP-GlcA



b) UDP-GlcA + UXS + NAD



c) UDP-GlcA + UXS

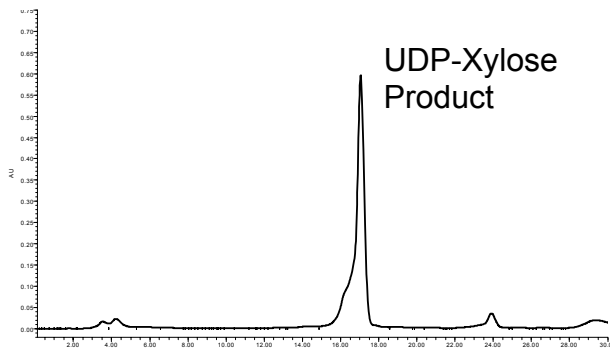
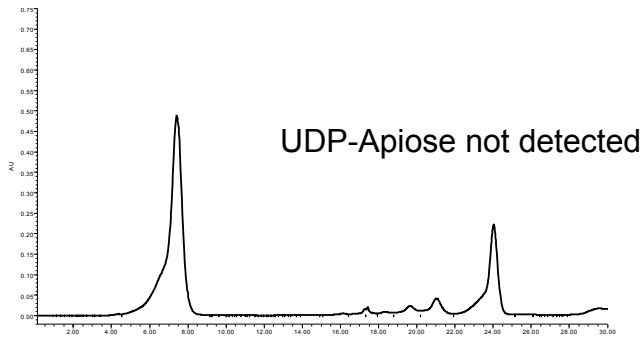


Fig.4.5: Results for HPLC based assays on UDP-GlcA decarboxylase (UXS) before fractionation. (a) UDP-GlcA standard (b) assay in presence of NAD, UXS & UDP-GlcA (c) assay in presence of UXS & UDP-GlcA only. The assays were repeated after fractionation (data not shown).

a) UDP-GlcA + NAD + UDP-Apiose synthase



b) UDP-GlcA + UDP-Apiose synthase

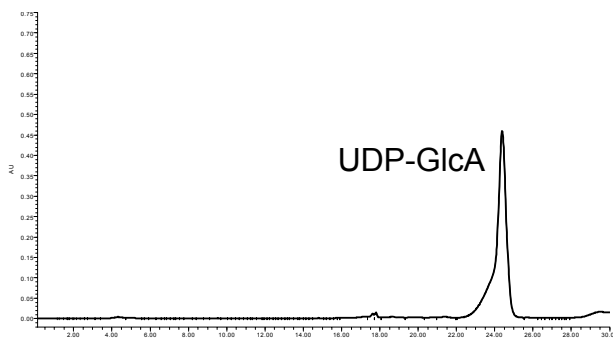
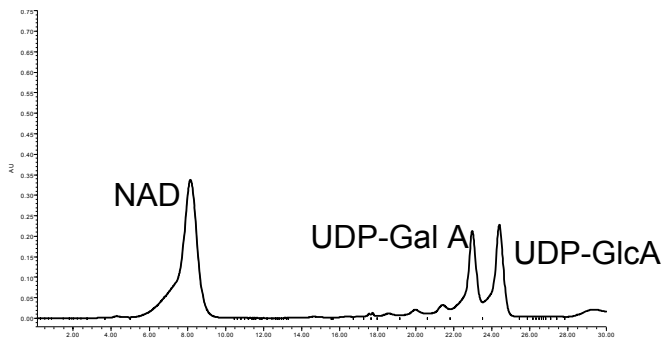


Fig.4.6: Results from HPLC based UDP-Apiose/Xylose synthase assays before fractionation. The assays were repeated also repeated after fractionation (data not shown). (a) UDP-Apiose is formed but could not be detected. (b) In absence of NAD no UDP-Apiose is formed. These assays demonstrate the importance of NAD for enzyme activity

a) UDP-GlcA + NAD + UDP-GlcA epimerase



b) UDP-GlcA + UDP-GlcA epimerase

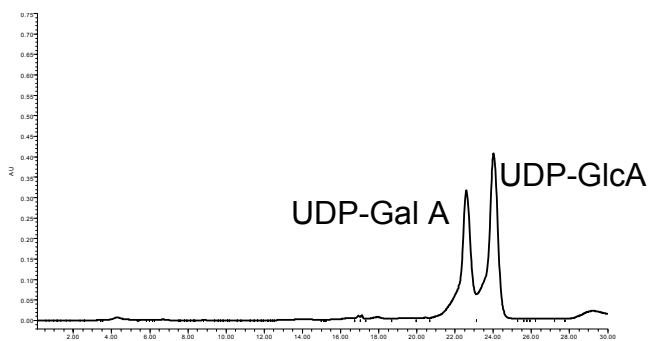
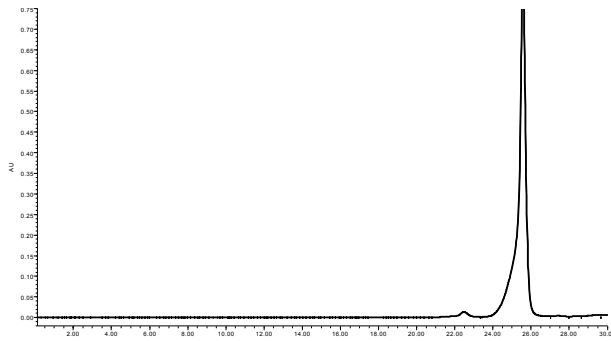


Fig.4.7: Results for HPLC based assays on UDP-GlcA epimerase before fractionation. (a) assay in presence of NAD, UDP-GlcA epimerase & UDP-GlcA (b) assay in presence of UDP-GlcA epimerase & UDP-GlcA only. The assays were repeated after fractionation (data not shown).

a) Standard ATP



b) Galk + Gal + ATP

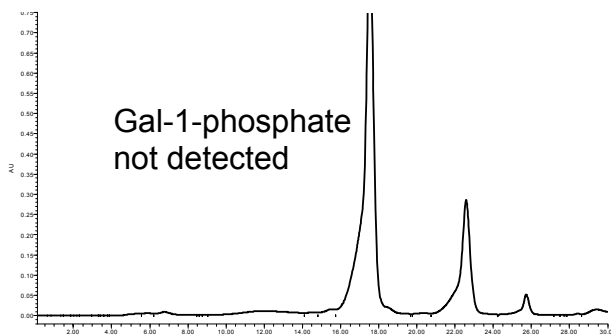


Fig.4.8: Results for HPLC based assays on Galk before fractionation. (a) ATP standard (b) Assay in presence of Galk, Gal & ATP. The product formed Gal-1-PO<sub>4</sub> is not detected by uv detector. However the reaction product ADP is detected. Ting from Dr. Maor's lab provided the enzyme which was used in the assay

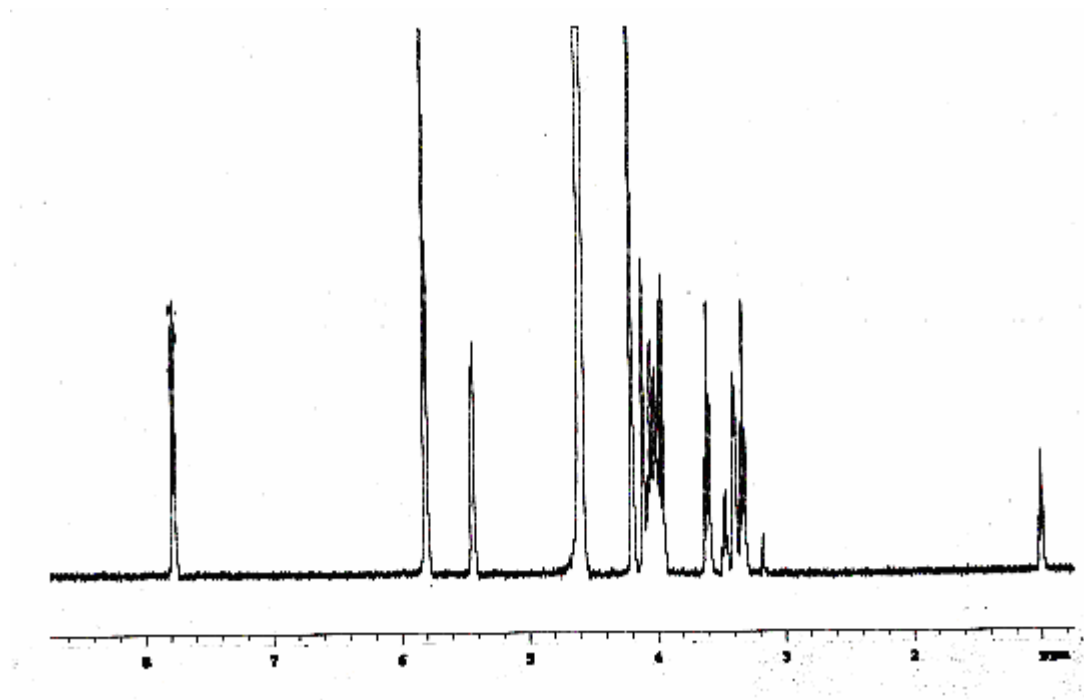


Fig.4.9:  $^1\text{H}$  NMR spectrum of 20 mM UDP-GlcA dissolved in  $\text{D}_2\text{O}$ . The acquisition parameters are relax. delay arrayed, Pulse 80.8 degrees, Acq. Time 2.048 sec, width 4000.0 Hz, 8 repetitions. Data was obtained using 500 MHz NMR instrument.

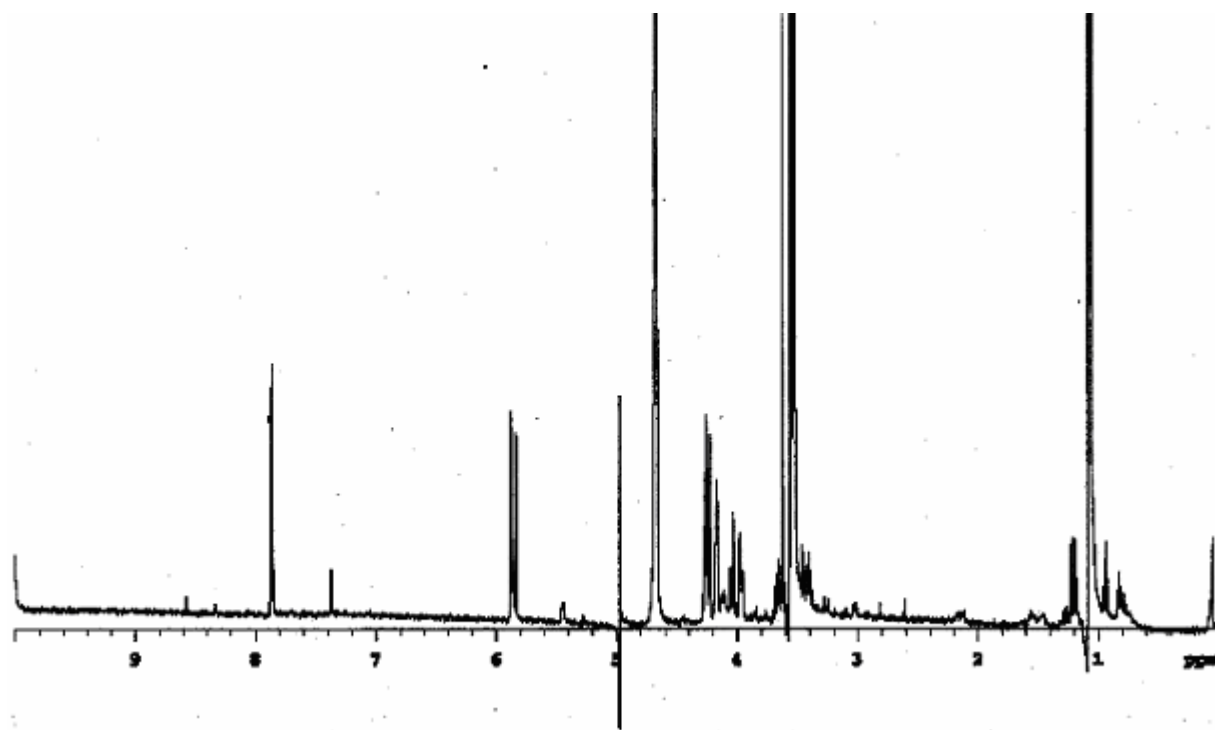


Fig.4.10:  $^1\text{H}$  NMR spectrum of UMP. Spectrum was provided by Dr. John Gluskha. The acquisition parameters are relax. delay arrayed, Pulse 80.8 degrees, Acq. Time 1.00 sec, width 5027.7 Hz, 4000 repetitions. Data was obtained using 500 MHz NMR instrument.

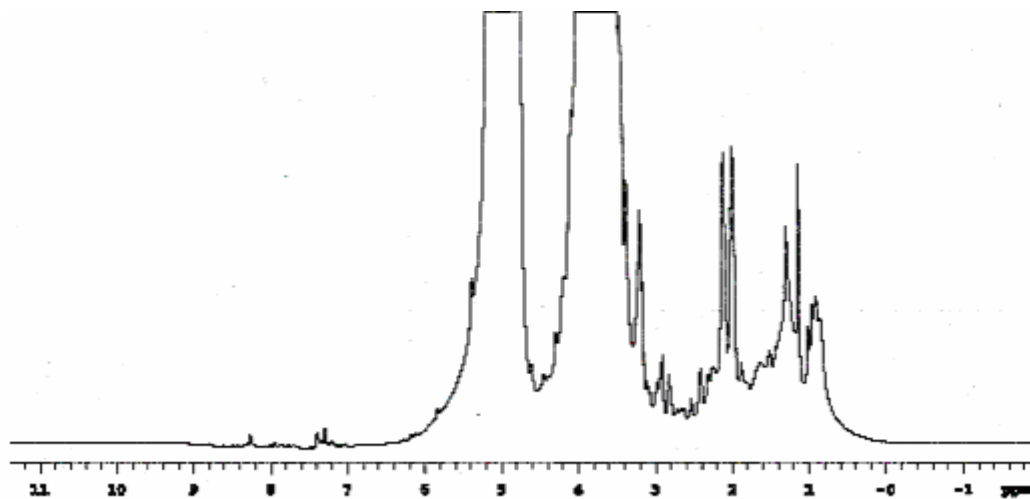


Fig.4.11:  $^1\text{H}$  NMR spectra collected  $\sim 0$  min after addition of 285  $\mu\text{l}$  pea Golgi + 15  $\mu\text{l}$  of  $\text{D}_2\text{O}$ . Spectra were collected with assistance from Dr. John Gluskha. The acquisition parameters are relax. delay arrayed, Pulse 80.8 degrees, Acq. Time 1.00 sec, width 8000.0 Hz, 1344 repetitions. Data was obtained using 600 MHz NMR instrument.

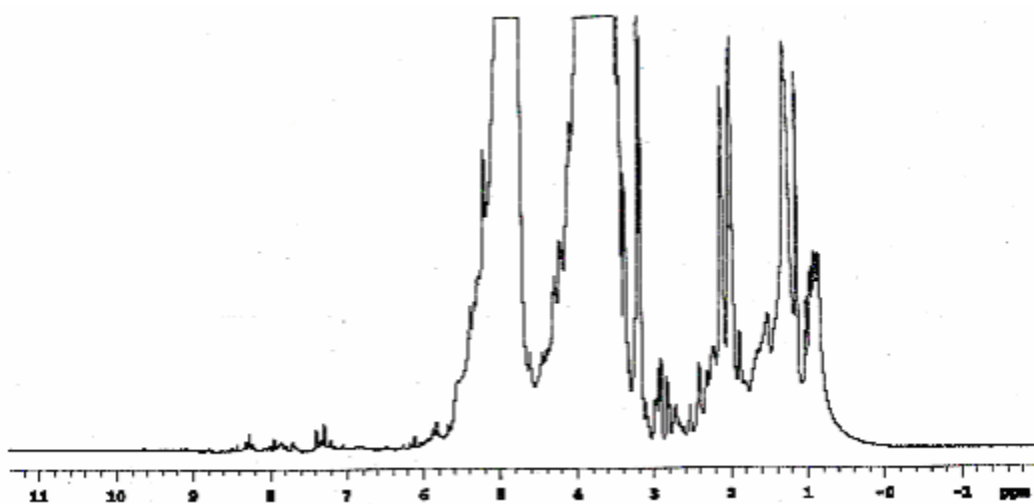


Fig.4.12:  $^1\text{H}$  NMR spectra collected ~ 7 hr after addition of 285  $\mu\text{l}$  pea Golgi + 15  $\mu\text{l}$  of  $\text{D}_2\text{O}$ . Spectra were collected with assistance from Dr. John Gluska. The acquisition parameters are relax. delay arrayed, Pulse 80.8 degrees, Acq. Time 1.00 sec, width 8000.0 Hz, 256 repetitions. Data was obtained using 600 MHz NMR instrument.

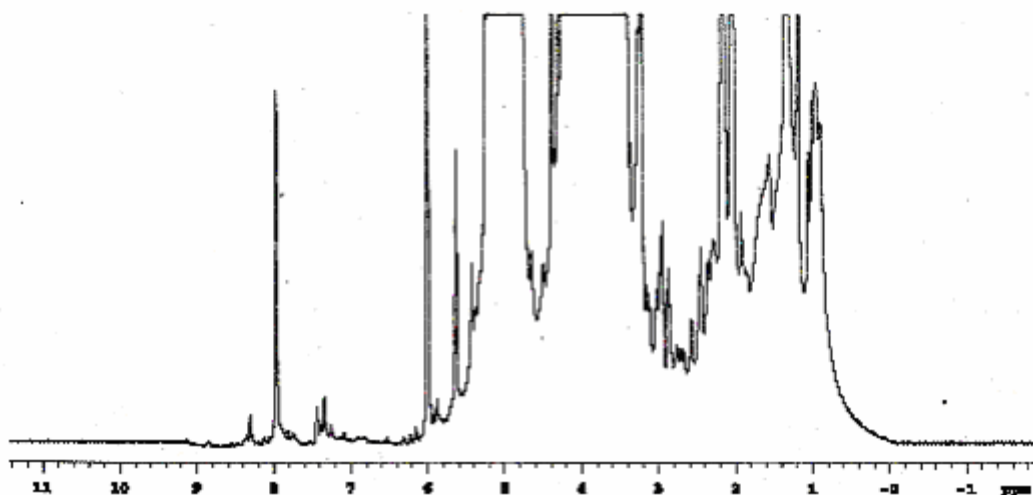


Fig.4.13: 285  $\mu$ l pea Golgi + 15  $\mu$ l of  $D_2O$ . To this mixture 30  $\mu$ l of 20 mM UDP-GlcA in  $D_2O$  was added after  $\sim$  1 hr and then an array of 10 spectra were collected for  $\sim$  1.5 hr. Spectra were collected with assistance from Dr. John Gluskha. The acquisition parameters are relax. delay arrayed, Pulse 80.8 degrees, Acq. Time 1.00 sec, width 8000.0 Hz, 256 repetitions. Data was obtained using 600 MHz NMR instrument.

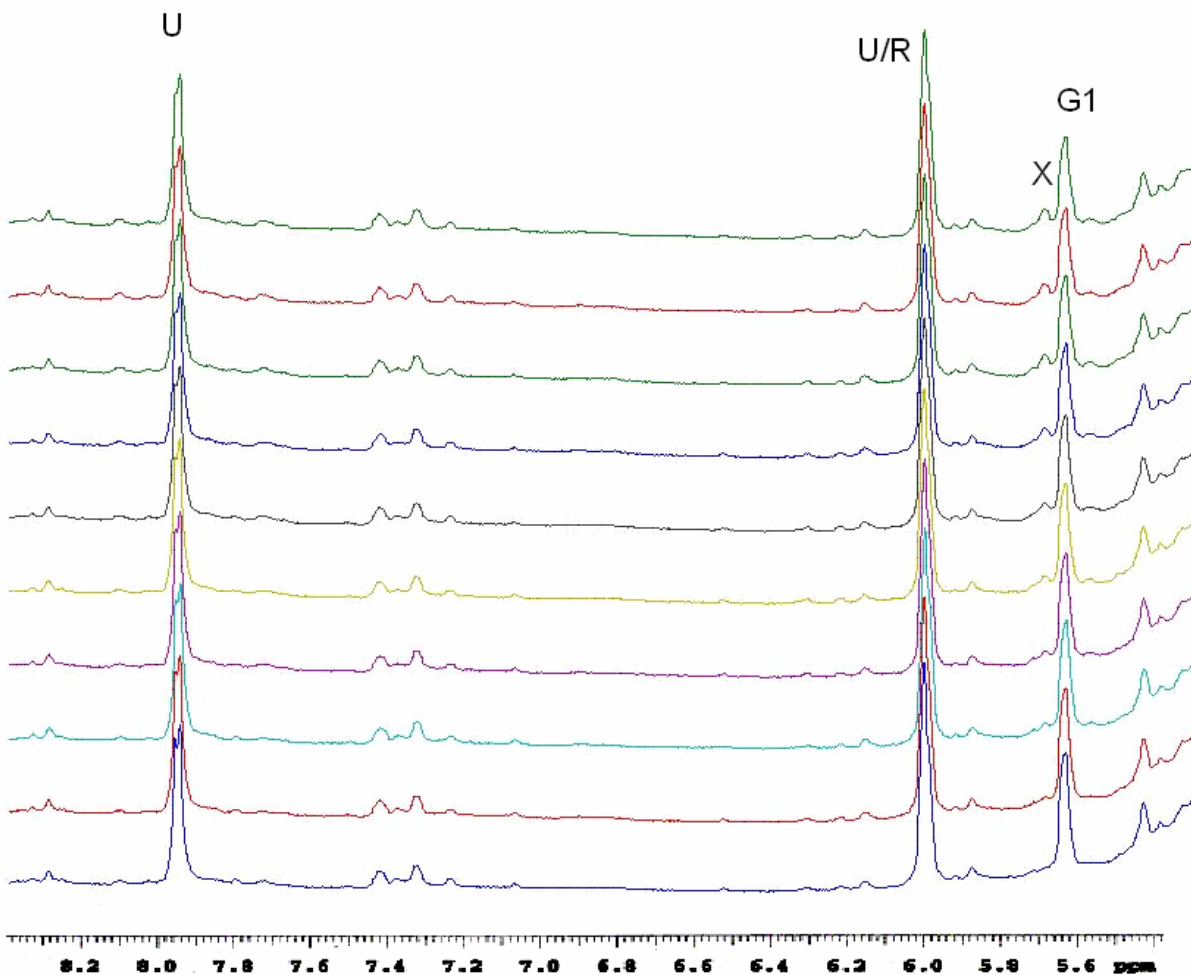


Fig.4.14: <sup>1</sup>H NMR spectrum showing the region between 5.5 – 8.3 ppm from figure 13. Peak G1 corresponds to proton at first position in Glucuronic acid, peaks labeled U correspond to uracil peaks whereas R corresponds to ribose in UDP-GlcA. The height of peak at G1 reduces over a period of time where as a new peak, X appears over that time period. (Data was processed in MATLAB)

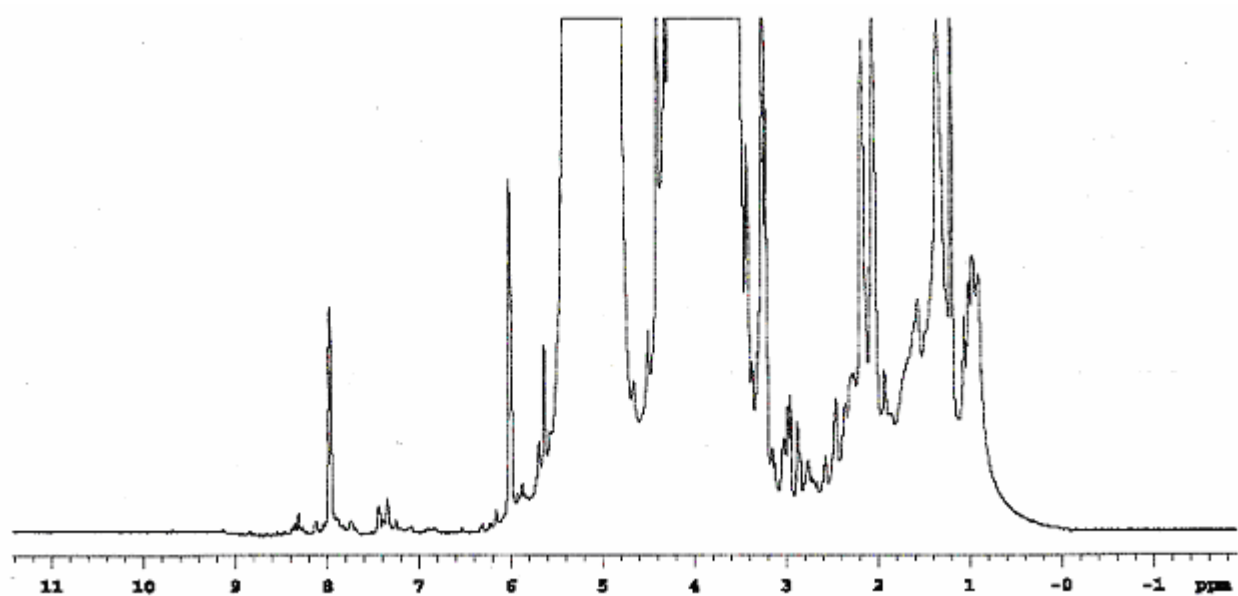


Fig.4.15: 285  $\mu\text{l}$  pea Golgi + 15  $\mu\text{l}$  of  $\text{D}_2\text{O}$ . To this mixture 30  $\mu\text{l}$  of 20 mM UDP-GlcA in  $\text{D}_2\text{O}$  was added after  $\sim 1$  hr. After  $\sim 2$ hr an array of 25 spectra were collected for  $\sim 3.5$  hrs. Spectra were collected with assistance from Dr. John Gluskha. The acquisition parameters are relax. delay arrayed, Pulse 80.8 degrees, Acq. Time 1.00 sec, width 8000.0 Hz, 256 repetitions. Data was obtained using 600 MHz NMR instrument.

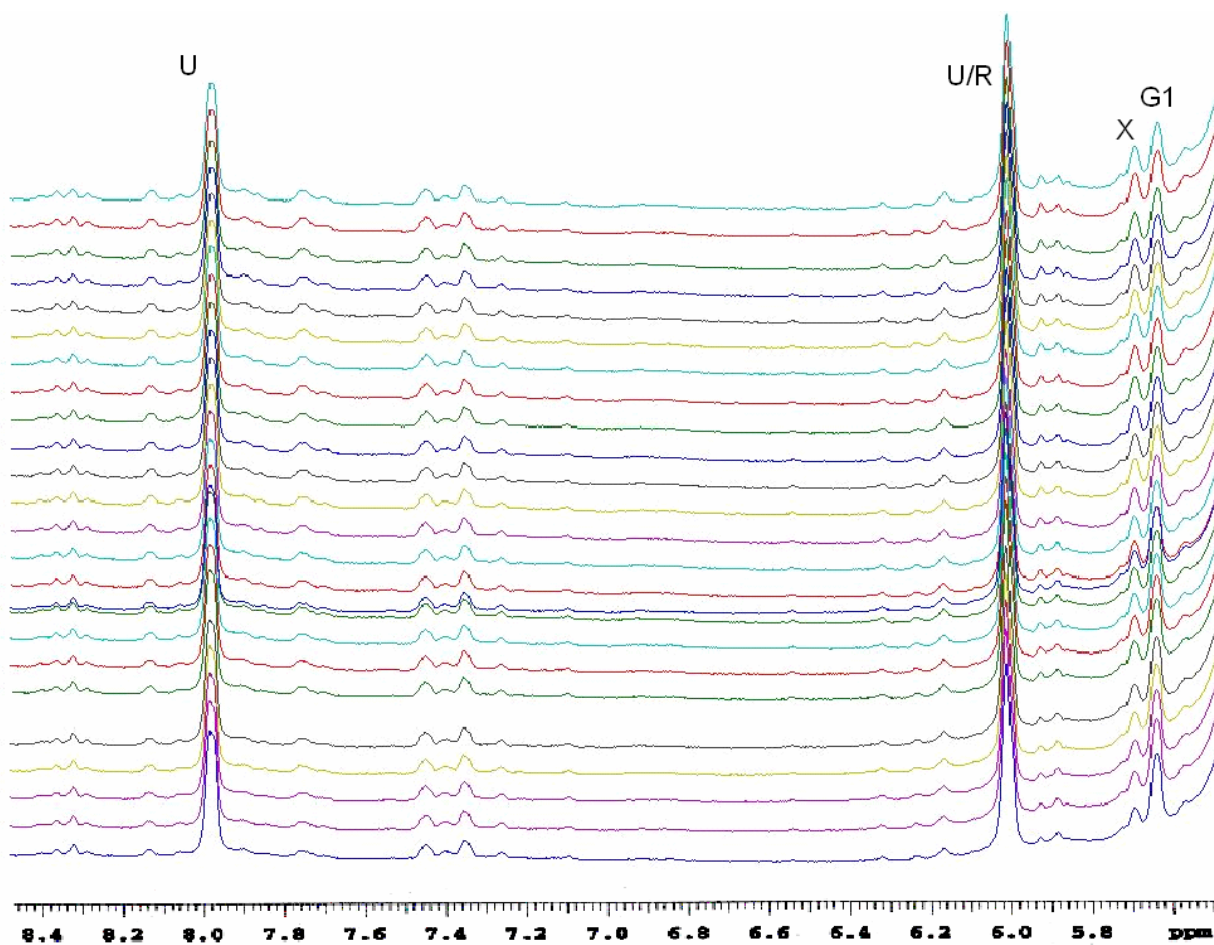


Fig.4.16:  $^1\text{H}$  NMR spectrum showing the region between 5.6 – 8.4 ppm from figure 15. Peak G1 corresponds to proton at first position in Glucuronic acid, peaks labeled U correspond to uracil peaks whereas R corresponds to ribose in UDP-GlcA. The height of peak at G1 reduces over a period of time whereas a new peak, X peak becomes prominent over that period. (Data was processed in MATLAB)

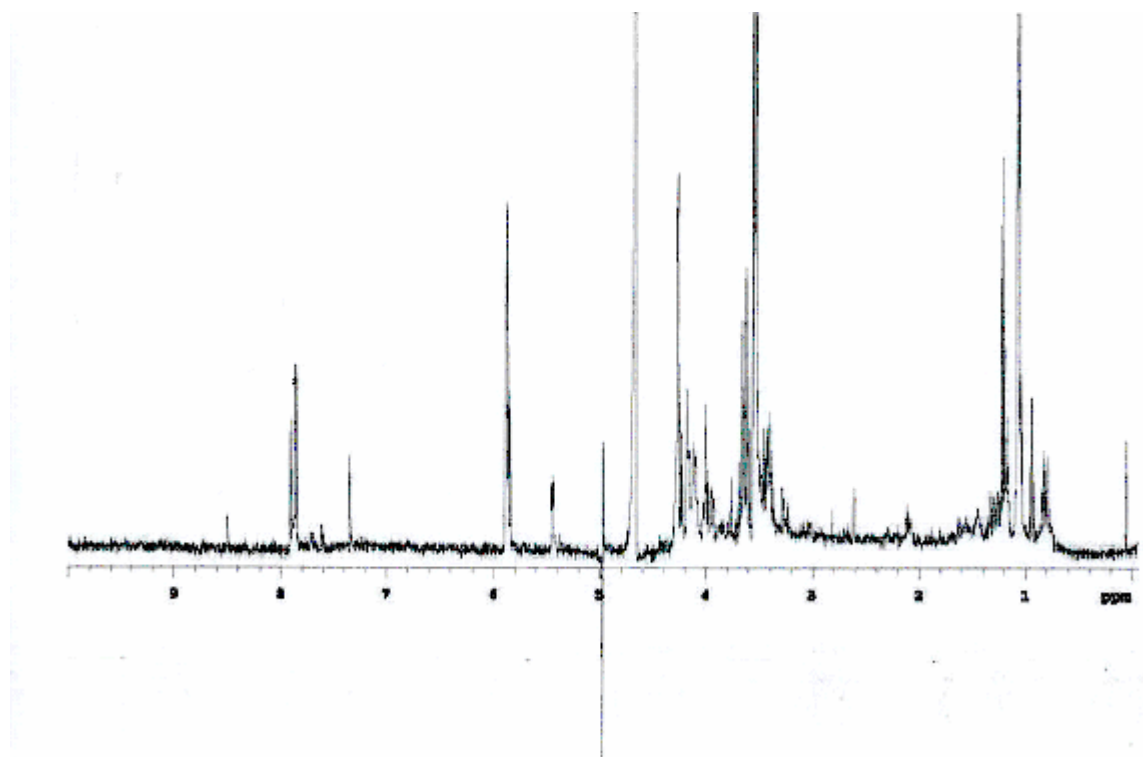


Fig.4.17:  $^1\text{H}$  NMR spectrum of UDP-Xylose. Spectra provided by Dr. John Glushka. The acquisition parameters are relax. delay 0.020 sec, Pulse 45 degrees, Acq. Time 1.00 sec, width 5027.7 Hz, 2272 repetitions. Data was obtained using 500 MHz NMR instrument.

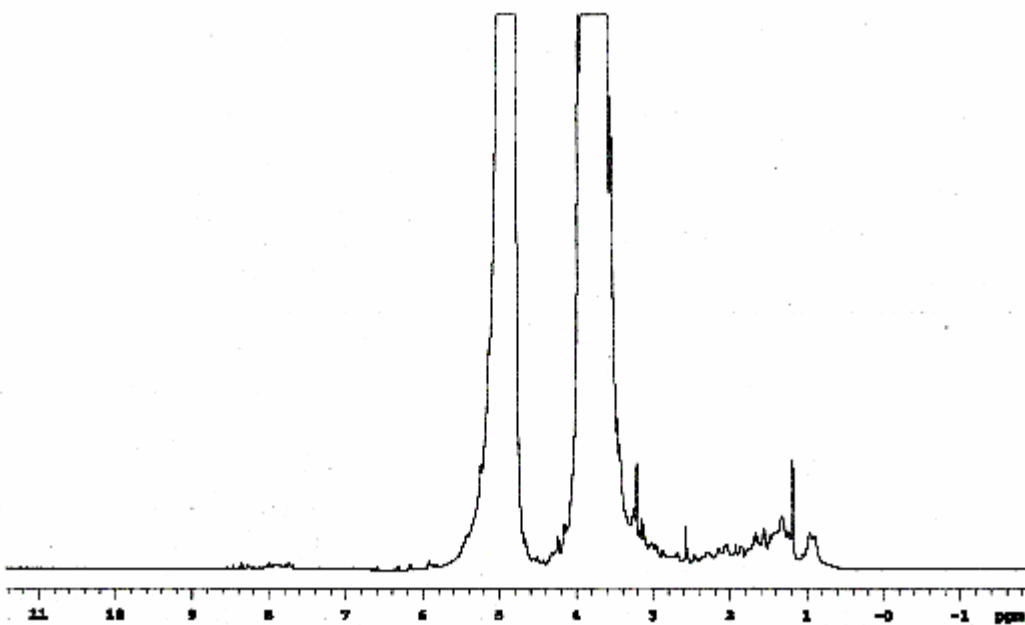


Fig.4.18:  $^1\text{H}$  NMR spectra collected  $\sim 0$  min after addition of 285  $\mu\text{l}$  maize Golgi + 15  $\mu\text{l}$  of  $\text{D}_2\text{O}$ . Spectra were collected with assistance from Dr. John Gluska. The acquisition parameters are relax. delay 0.020 sec, Pulse 80.8 degrees, Acq. Time 1.00 sec, width 8000.0 Hz, 288 repetitions. Data was obtained using 600 MHz NMR instrument.

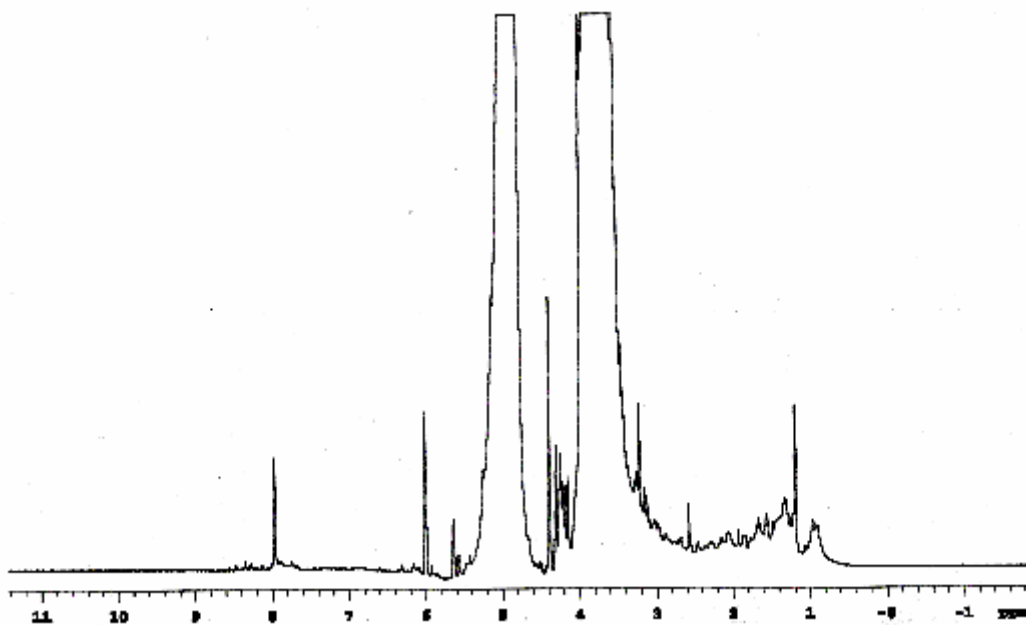


Fig.4.19:  $^1\text{H}$  NMR spectra collected  $\sim 0$  min after addition of 285  $\mu\text{l}$  maize Golgi + 15  $\mu\text{l}$  of  $\text{D}_2\text{O}$  + 30  $\mu\text{l}$  of 20 mM UDP-GlcA. Spectra were collected with assistance from Dr. John Gluska. The acquisition parameters are relax. delay 0.020 sec, Pulse 80.8 degrees, Acq. Time 1.00 sec, width 8000.0 Hz, 256 repetitions. Data was obtained using 600 MHz NMR instrument.

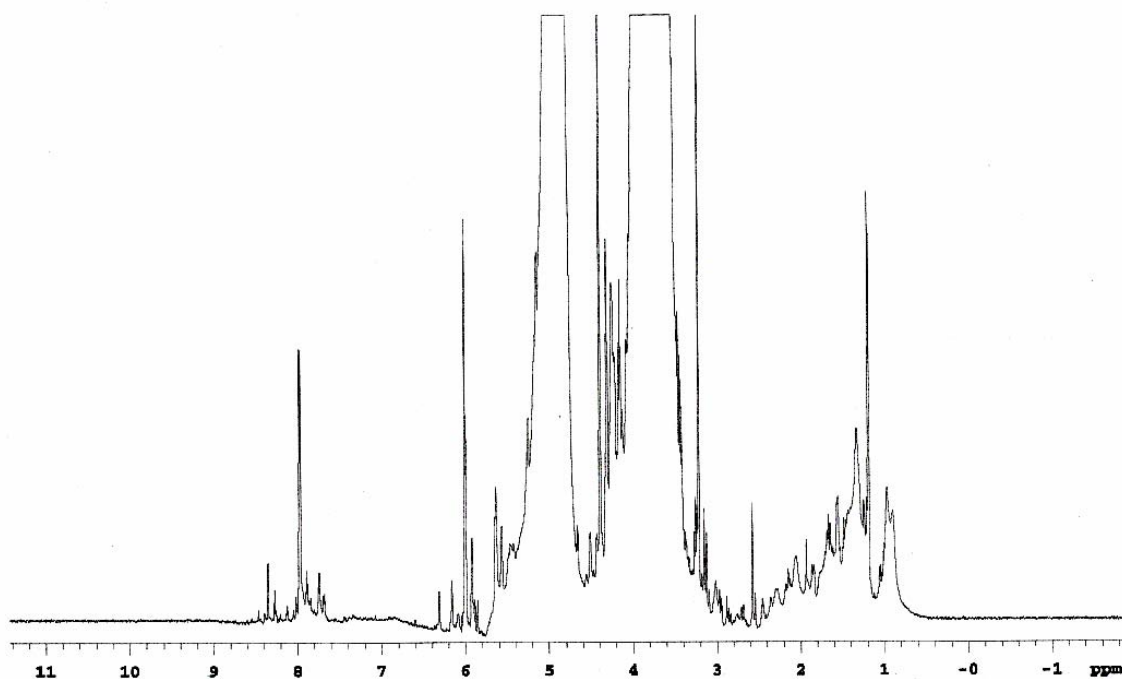


Fig.4.20:  $^1\text{H}$  NMR spectra collected ~ 5 hr after addition of 285  $\mu\text{l}$  maize Golgi + 15  $\mu\text{l}$  of  $\text{D}_2\text{O}$  + 30  $\mu\text{l}$  of 20 mM UDP-GlcA. Spectra were collected with assistance from Dr. John Gluska. The acquisition parameters are relax. delay 0.020 sec, Pulse 80.8 degrees, Acq. Time 1.00 sec, width 8000.0 Hz, 256 repetitions. Data was obtained using 600 MHz NMR instrument.

## APPENDIX A

### Matlab Program to generate Hilbert-transform matrix

```
t = ' 1 / ( i + j -1)';  
for j = 1:n  
    for i = 1:n  
        a(i, j) = eval(t);  
    end  
end  
end
```

This generates m-by-n Hilbert transform matrix. The code is taken from MATLAB manual

## APPENDIX B

### Matlab Commands

1. Transpose: If A is a matrix then transpose of A is obtained from command A'
2. Addition/subtraction: If A and B are two matrices having same dimensions, then

$$C = A + B \text{ (addition)}$$

$$D = A - B \text{ (subtraction)}$$

3. Multiplication: If A and B are two matrices, then

$$E = A * B \text{ (multiplication)}$$

This operation is possible provided if the second dimension of A is same as the first dimension of B

$$F = A.*B$$

The resultant of this operation denotes array, or element-by-element multiplication between matrices A and B

3. Generating a larger matrix: If A (3 x 3) and B (1 x 3) are two matrices, then

$$G = [A; B] \text{ (generates a 4 x 3 matrix)}$$

4. Extract smaller matrix: If A (4 x 3) matrix, then

H = A(1:3, :) (generates a 3 x 3 matrix which takes first three rows and all columns of A)

H1= A(1:4,1); H2 = A(1:4,2) & H3 = A(1:4,3) (where resultant H1, H2 & H3 extracts column 1, 2 and 3 respectively from the matrix A)

5. Singular value decomposition: For a square matrix, A

$$[u, s, v] = \text{svd}(A)$$

where the resultant  $u$  correspond to the eigen vectors,  $v$  correspond to the eigen values and  $s$  is the diagonal matrix.

6. Contour plot: For a matrix,  $A$

`contour(A)` (draws a contour plot of matrix  $A$ . The matrix  $A$  must be at least  $2 \times 2$  matrix containing at least two different values

`contour(A,n)` (contour plot of matrix  $a$  with  $n$  contour levels)

7. Random number generation:

`A = rand(50,1)` ( generates a matrix  $A$  with 50 random numbers between 0 and 1 in a single column)

`A = rand(1, 50)` ( generates a matrix  $A$  with 50 random numbers between 0 and 1 in a single row)

These commands are taken from MATLAB manual

## APPENDIX C

### Write spec macro

(write a portion of a spectrum into an ASCII file)

writespec('filename') writes the spectrum from sp+wp to sp into a file in an ASCII format

```
if ($#<1) then
    write('error', 'usage: writespec(\`filename\`')
else
    mark('reset')
    write('line3', 'creating file %s...', $1)
    write('reset', $1)
    $delta=sw/(fn/2-1) $f=sp+wp
    repeat
        mark($f):$ht
        write('file', $1, '%f', $ht)
        $f=$f-$delta
    until $f<sp
    write('error', 'Done!')
endif
```

This macro is taken from Varian VnmrJ software